# Rapid tolerance to morphine in the myenteric neurons of the small intestine is independent of β-arrestin-2

Karan H. Muchhala[1], Joanna C. Jacob[1], Imran Alam[1], Shahzeb Hasan[1], Aliyeen Khan[1], Minho Kang[1], William L. Dewey[1] and Hamid I. Akbarali[1*].

1. Department of Pharmacology and Toxicology, Virginia Commonwealth University, 1112 East Clay St, Richmond, VA 23298, USA

**Correspondence:** Hamid I. Akbarali, PhD

Department of Pharmacology and Toxicology, Virginia Commonwealth University

1112 East Clay Street, Richmond, VA 23298, USA

Phone: 804-828-9688

Email: hamid.akbarali@vcuhealth.org

**Abstract**

The differential rates of opioid tolerances raise the question of discrete underlying mechanisms. While opioid tolerance is strongly linked to the development of dependence, there is a dissociation between the two phenomena in the gut as tolerance does not develop to chronic opioid-induced constipation, but diarrhea still manifests upon withdrawal. Here, we find that tolerance develops to inhibition of small intestinal motility after one day of morphine exposure, and is more rapid compared to spinally-mediated antinociception and constipation in chronic morphine-treated mice. This tolerance can be reversed by protein kinase C (PKC) inhibition but not by β-arrestin-2 deletion. Similarly, morphine tolerance develops to inhibition of neuronal excitability in ileum myenteric neurons independently of β-arrestin-2 and is attenuated by inhibiting PKC. These findings reveal a potential mechanism for differences in the rates of tolerances to opioids and implicate myenteric neurons of the ileum as the primary cause for opioid-induced withdrawal effects.

34 **Introduction**

35 It is well known that there are differences in the rates and extent of tolerance development in various
36 tissues to opioids. Tolerance develops to the desired analgesic effects of opioids at a faster rate than to
37 the undesired respiratory depression and constipation, which ultimately limits the applicability of
38 opioids to treat chronic pain (Hayhurst and Durieux, 2016). The differential rate of tolerance
39 development to opioids, thus raises the question of differences in the mechanisms leading to tolerance.

40 It is now well established that most G protein-coupled receptors (GPCRs) undergo dynamic changes in
41 receptor confirmation to engage multiple transducers and modulatory proteins with distinct efficacies
42 (Kenakin, 2011; Rajagopal *et al.*, 2011; Flock *et al.*, 2017; Latorraca *et al.*, 2017; Hilger *et al.*, 2018). This
43 is the basis of the concept of "biased agonism" or "functional selectivity". Fundamentally, biased
44 agonists induce ligand-specific changes in the confirmation of GPCRs and cognate transducers to
45 exclusively activate associated downstream effector systems (Michel and Charlton, 2018; Wootten *et*
46 *al.*, 2018). The phenomenon of biased agonism has also been described for the μ-opioid receptor (MOR),
47 which mediates the clinical effects of morphine and other opioid analgesics.

48 MOR is a $G\alpha_{i/o}$-coupled GPCR, which can also engage multi-functional adaptor proteins called β-
49 arrestins. Classically, β-arrestins function to attenuate G protein-mediated signal transduction of GPCRs
50 by sterically obstructing G protein binding to the activated receptor. Alternately, β-arrestins are also
51 known to initiate G protein-independent signal transduction once bound to the receptor (Lohse *et al.*,
52 1990; Lefkowitz, 1998). Previous studies have shown that genetic deletion of β-arrestin-2 (βarr2) or
53 down-regulation of β-arrestin-2 results in reduced antinociceptive tolerance to morphine in rodents
54 (Bohn *et al.*, 1999, 2000; Yang *et al.*, 2011; Wang *et al.*, 2016). These studies suggest that β-arrestin-2 is
55 necessary for MOR-mediated cellular processes underlying antinociceptive tolerance to opioids. This "β-
56 arrestin-2 hypothesis" was further supported by studies, which used MOR biased agonists that

57 preferentially activate G proteins over β-arrestin-2 and found reduced antinociceptive tolerance
58 compared to morphine (DeWire *et al.*, 2013; Manglik *et al.*, 2016; Grim *et al.*, 2020).

59 In the gastrointestinal (GI) tract, it was previously reported that knock out of β-arrestin-2 results in a
60 phenotype that is more resistant to opioid-induced inhibition of GI motility (Raehal *et al.*, 2005). On this
61 basis, the authors postulated that activation of β-arrestin-2-mediated signal transduction underlies
62 opioid-induced constipation (Raehal *et al.*, 2005). However, a number of different strategies to induce G
63 protein-biased signal transduction at the MOR in later studies, such as the use of β-arrestin-2 knock out
64 mice, phosphorylation-deficient MOR knock-in mice or biased agonists (TRV130 and PZM21), failed to
65 mitigate opioid-induced GI dysfunction (Kang *et al.*, 2012; Maguma *et al.*, 2012; Manglik *et al.*, 2016;
66 Altarifi *et al.*, 2017; Kliewer *et al.*, 2019). Furthermore, it was observed that chronic exposure to
67 morphine induced down-regulation of β-arrestin-2 in the ileum, but levels in the colon remained
68 unchanged. Moreover, deletion of β-arrestin-2 induced morphine tolerance in the colon, which under
69 control experimental conditions did not become tolerant to morphine (Ross *et al.*, 2008; Kang *et al.*,
70 2012; Maguma *et al.*, 2012). Thus, unlike in pain pathways where β-arrestin-2 is required for the
71 development of analgesic tolerance, tolerance to motility in the colon could be induced by
72 circumventing the β-arrestin-2 pathway. In contrast, the isolated ileum tissue developed tolerance to
73 morphine irrespective of the absence or presence of β-arrestin-2 (Ross *et al.*, 2008; Kang *et al.*, 2012;
74 Maguma *et al.*, 2012). Consequently, the data suggested that β-arrestin-2 might mediate tolerance in
75 the colon but the role of this multifunctional protein remains unknown in the development of morphine
76 tolerance in the ileum, specifically in neuronal substrates that regulate motility in the ileum.

77 Opioid tolerance is considered to induce physical dependence (Cox, 1999). Diarrhea is a common
78 adverse effect associated with physical dependence (Wesson and Ling, 2003; Donroe *et al.*, 2016) and
79 can be caused by withdrawal-induced changes in motor and secretomotor activities of the enteric

80 nervous system (Collier *et al.*, 1981; Warhurst *et al.*, 1984; Bianchetti *et al.*, 1986; Johnson *et al.*, 1987;
81 Smith *et al.*, 2014). We have previously shown that tolerance develops to repeated morphine exposure
82 in the isolated ileum but not in the colon (Ross *et al.*, 2008; Kang *et al.*, 2012; Maguma *et al.*, 2012) and
83 that in myenteric plexus neurons, which are known to regulate gastrointestinal peristalsis, naloxone
84 induced hyperexcitability in those isolated from the ileum but not the colon of morphine-tolerant mice
85 (Furness *et al.*, 2014; Smith *et al.*, 2014). Given these findings, it is possible that withdrawal-induced
86 diarrhea might be an ileum-derived effect. Since novel biased agonists at the MOR are being developed
87 for clinical use with the promise of desired analgesia without the unwanted adverse effects, it is
88 important to delineate the mechanism of tolerance in the ileum, specifically the role of the β-arrestin-2
89 desensitization pathway.

90 The present study shows that, unlike antinociceptive tolerance, which is purportedly mediated by β-
91 arrestin-2, morphine tolerance to small intestinal transit and in myenteric plexus neurons is mediated by
92 a protein kinase C (PKC)-dependent mechanism that does not involve the β-arrestin-2 pathway.
93 Furthermore, we find that morphine tolerance to small intestinal transit manifests before tolerance to
94 antinociception and whole gastrointestinal transit. In conclusion, the present study suggests that distinct
95 rates of morphine tolerance might be due to differences in the role of β-arrestin-2 in the mechanism of
96 tolerance at the MOR. Furthermore, the findings presented here raise the possibility that G-protein
97 biased agonists might induce tolerance in the ileum and lead to the development of physical
98 dependence even if tolerance to antinociception is prevented.

99 **Results**

100 **Establishing a model of morphine tolerance in male and female mice**

101 We first established a paradigm that produced *in vivo* morphine tolerance in male and female mice. For
102 this purpose, we initially tested morphine dose-response in both male and female βarr2 WT mice
103 implanted with 25 mg morphine (or placebo) pellet for 7 days. As shown in Figure 1A., there was a
104 significant rightward shift in the cumulative morphine dose response relationship of morphine-pelleted
105 βarr2 WT female mice compared to that of placebo-pelleted mice (Fig. 1A; Table S1). Repeated
106 measures three-way ANOVA with Tukey's post hoc test found a statistically significant difference in the
107 %MPE of placebo and morphine-pelleted female mice at 4, 8, 16 and 32 mg/kg doses of morphine (Fig.
108 1A; Table S1). In contrast, the cumulative dose response curves of 25 mg morphine-pelleted and
109 placebo-pelleted male mice were not significantly different from each other (Fig. 1A; Table S1). The
110 $ED_{50}$ values of placebo-pelleted and 25 mg morphine- pelleted βarr2 WT male mice, 2.18 (1.7 - 2.78)
111 mg/kg and 3.23 (2.26 - 4.62) mg/kg respectively, overlapped, indicating that the potency shift was not
112 significant. Furthermore, repeated measures three-way ANOVA with Tukey's post hoc test indicated that
113 there was no statistically significant difference in the %MPE of placebo and morphine-pelleted male
114 mice at any test dose of morphine (Fig. 1A; Table S1). Thus, while 7 days of exposure to 25 mg morphine
115 pellet induced tolerance in female mice, it was not sufficient to produce tolerance in male mice in the
116 warm-water tail-withdrawal assay.

117 To induce tolerance in male βarr2 mice, 2 x 25 mg (50 mg) morphine pellets for 7 days were used. The
118 cumulative morphine dose response curve of male βarr2 WT mice was significantly right-shifted
119 compared to placebo controls (Fig. 1B). Analysis by repeated measures two-way ANOVA revealed
120 significant differences between placebo and morphine-pelleted βarr2 WT male mice at several doses

121 (Fig. 1B; Table S1). Thus, 7-day treatment with 50 mg morphine produced tolerance to morphine-
122 induced antinociception in the warm-water tail-withdrawal assay.

123 These data suggest that sex differences exist in the development of tolerance to morphine in the βarr2
124 C57/Bl6 mice. The following experiments were therefore carried out using 25 mg and 50 mg (2 x 25 mg)
125 morphine pellets in female and male mice, respectively.

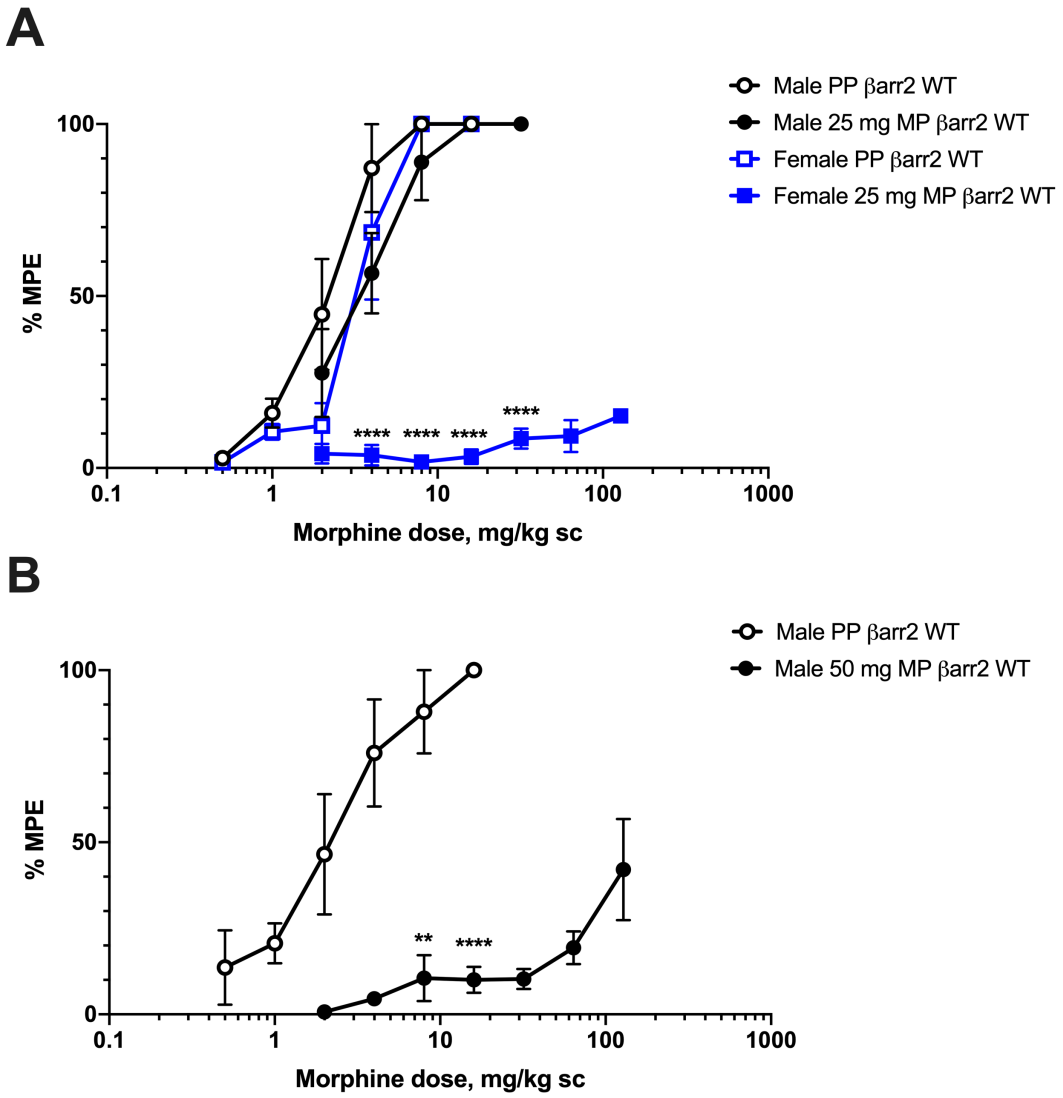


**Figure 1. Cumulative dose response curves in morphine-pelleted male and female mice.** (A) Antinociceptive tolerance produced by 7-day 25 mg morphine pellet in male and female mice was compared in the warm-water tail-withdrawal assay (56$^{o}$C). 25 mg morphine pellet produced a significant right-shift in the morphine dose response curve of female mice, but not male mice, compared to placebo controls. Data are mean ± SEM. Males: N=5/group for PP WT and 25 mg MP WT. Females: N=4/group for PP WT and 25 mg MP WT. ****P<0.0001 (versus female PP WT) by repeated measures three-way ANOVA with Tukey's post hoc test. (B) The morphine dose response curve of male mice was significantly right-shifted from placebo when they were pelleted with 50 mg morphine for 7 days. Data are mean ± SEM. N=6/group. **P<0.01 and ****P<0.0001 (versus male PP WT) by repeated measures two-way ANOVA with Sidak's test.

126 **Morphine tolerance in ileum myenteric plexus neurons is not contingent on the β-arrestin-2-**
127 **desensitization pathway**

128 As noted previously, tolerance to repeated morphine in the isolated ileum tissue is not dependent on
129 the presence of β-arrestin-2 (Kang *et al.*, 2012). In order to determine if tolerance could manifest in
130 isolated neurons, whole-cell patch clamp electrophysiology in the current-clamp mode was used. For
131 this purpose, ileum myenteric plexus neurons harvested from β- arrestin-2 WT and KO male mice were
132 exposed to morphine *in vitro* (10 µM morphine for 15-18 hours) or *in vivo* (50 mg morphine pellet for 7
133 days) and cellular tolerance was assessed by monitoring changes in neuronal excitability in response to
134 acute morphine (3 µM) challenge (Figs. 2, 3). Threshold potential, which is the membrane potential at
135 which action potential is elicited, was used as the primary metric of neuronal excitability. Threshold
136 potential increase from baseline signified reduced neuronal excitability. Cellular tolerance was described
137 as the failure of the acute morphine challenge dose to alter threshold potential.

138 Acute exposure to 3 µM morphine increased the threshold to fire action potential in naïve βarr2 WT
139 ileum neurons (-20.8 ±3.8 mV to -15.3 ±4.3 mV), but not in neurons previously exposed to morphine *in*
140 *vitro* (-21.9 ±1.6 mV to -23.1 ± 0.9 mV) or *in vivo* (-25.1 ±1.8 mV to -26.4 ±1.7 mV), indicating cellular
141 tolerance development (Figs. 2, 3A, 3B and Tables 2 and S1). The shift in threshold potential in naïve WT
142 neurons was time-dependent with a significant increase from baseline observed after 4 minutes of 3 µM
143 morphine exposure ($P<0.05$; Fig. 3B and Table S1). Neurons previously exposed to morphine did not
144 produce significant deviation in threshold potential from baseline over the course of 16 minutes
145 ($P>0.05$; Fig. 3B and Table S1).

146 In ileum neurons from β-arrestin-2 KO mice, threshold potential was depolarized following acute
147 morphine challenge (-25.0 ±1.5 mV to -19.5 ±1.7; Figs. 3C and 3D), indicating that depletion of β-
148 arrestin-2 did not disrupt the ability of the MOR to respond to acute morphine. Acute morphine-induced

149 change in threshold potential was time-dependent with significant increase from baseline observed
150 after 6 minutes ($P<0.05$; Fig. 3D). 3 µM morphine produced a similar increase in threshold potential in
151 WT and KO neurons (WT: 5.6 ±1.0 mV, KO: 5.5 ±0.5 mV; Fig. 3E). No significant deviation in threshold
152 potential from baseline was observed in *in vitro* (-22.1 ±2.1 mV to -23.6 ±2.6 mV) or *in vivo* (- 22.4 ±2.0
153 mV to -21.5 ±2.6 mV) morphine-treated β-arrestin-2 knock out neurons following acute morphine
154 challenge (Figs. 3C and 3D; Table 2). The lack of response to the acute morphine challenge persisted for
155 16 minutes (Fig. 3D), indicating morphine tolerance in β-arrestin-2 knock out neurons (Table S1). Acute
156 exposure to morphine did not alter the resting membrane potential of naïve (WT: - 45.1 ±3.0 mV to -
157 45.3 ±3.3 mV; KO: -52.7 ±2.5 mV to -53.4 ±3.9), *in vitro* (WT: - 45.4 ±1.9 mV to -49.7 ±0.8 mV; KO: -
158 54.4 ±4.5 mV to -53.7 ±4.5 mV) or *in vivo* (WT: -57.5 ±2.2 mV to -55.7 ±1.8 mV; KO: -51.5 ±2.6 mV to -
159 51.8 ±4.1 mV) morphine-treated ileum neurons with or without β-arrestin-2 (Table 2).

160 Thus, depletion of β-arrestin-2 does not mitigate tolerance in ileum neurons and cellular tolerance to
161 morphine develops in ileum neurons independent of the βarr2-desensitization pathway.

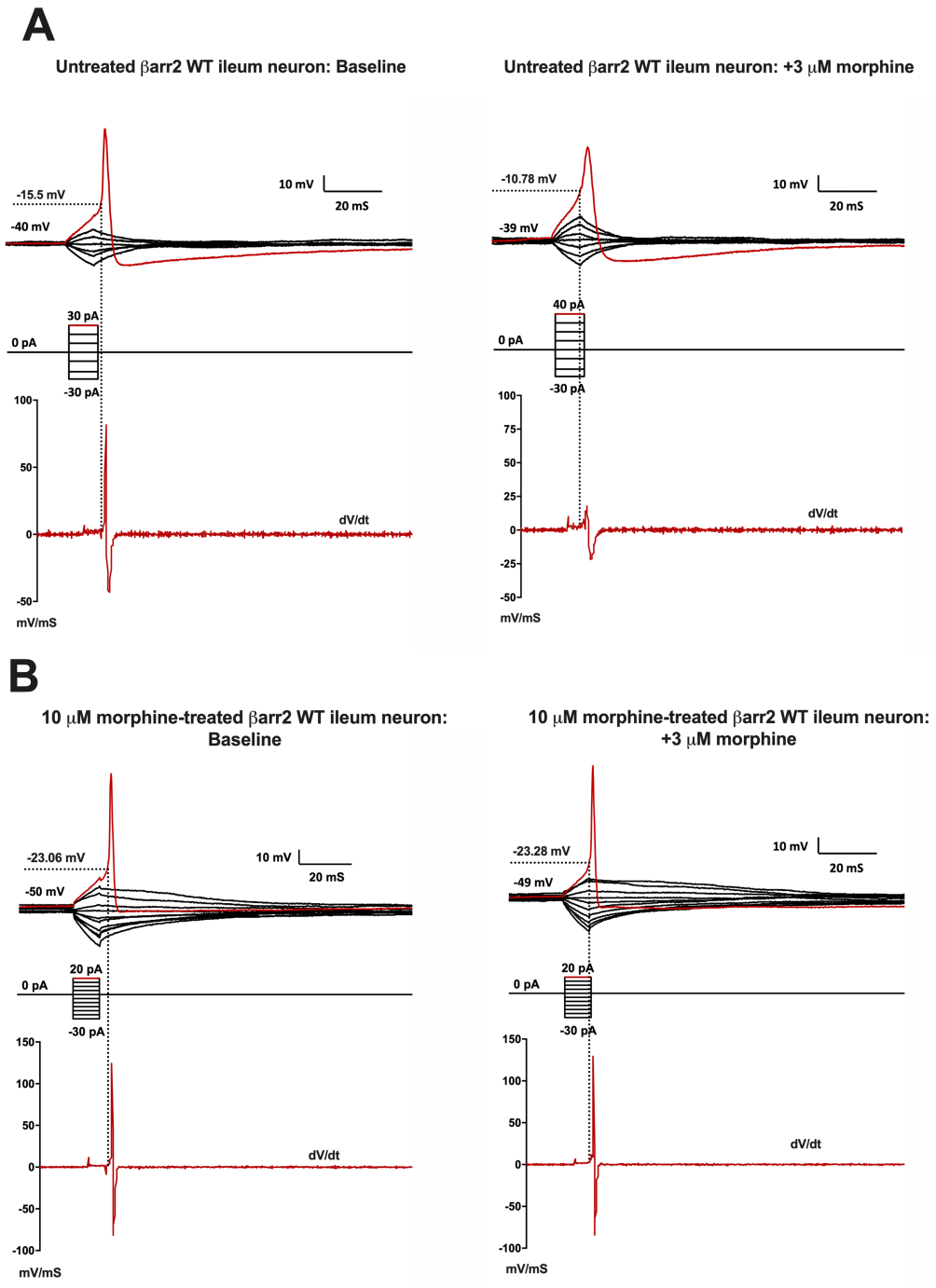


**Figure 2. Representative current-clamp traces of untreated and 10 μM morphine-treated βarr2 WT ileum neuron before and after acute morphine challenge demonstrating the measurement of threshold potential.** Whole-cell current clamp traces of (A) untreated or (B) 10 μM morphine-treated (*in vitro*-treated) βarr2 WT ileum myenteric neuron at baseline (left) and after 16 minutes of acute 3 μM morphine (right). Action potential (top; in red) generated by a step-wise current stimulation protocol (middle) with the first stimulus to elicit action potential is marked in red. Threshold potential (dotted line), which is a measure of neuronal excitability, is extrapolated from the point on the action potential

derivative trace (bottom), where dV/dt>0. Acute treatment with 3 µM morphine increased threshold potential of untreated βarr2 WT neuron, but not of the 10 µM morphine-treated cell.

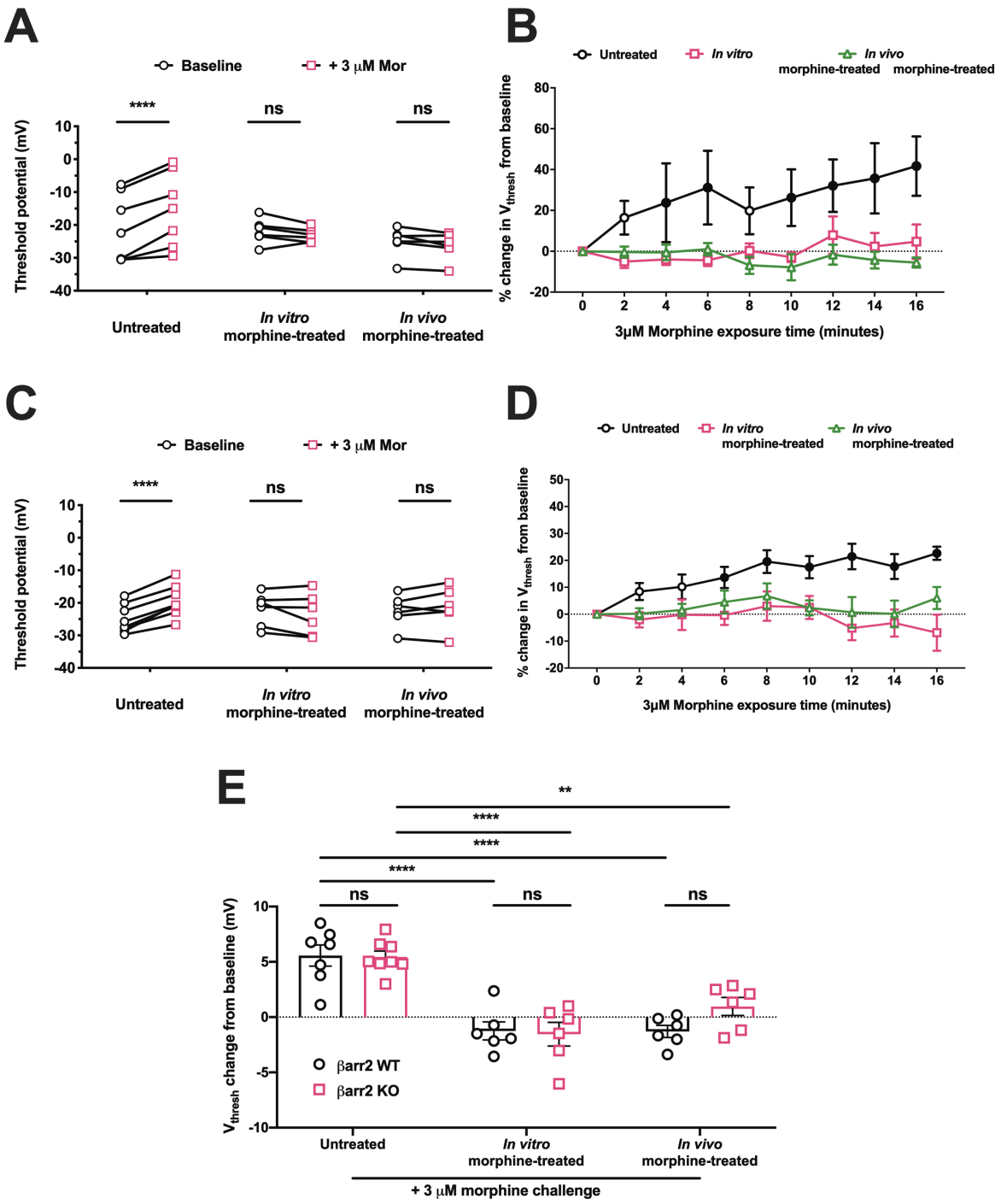


**Figure 3. Morphine tolerance in ileum myenteric plexus neurons does not depend on β-arrestin-2.** Ileum myenteric plexus neurons from male (A and B) βarr2 WT or (C and D) KO mice were bath perfused with 3 μM morphine and the change in $V_{thresh}$ was monitored for up to 16 minutes. (A and C) Threshold potential before (baseline) and after 3 μM morphine in individual (A) βarr2 WT or (C) βarr2 KO neurons. *P<0.05, ***P<0.001 and 'ns' (not significant, P>0.05) by two-way repeated-measures ANOVA with Sidak's post hoc test. (B and D) Time course of percent threshold potential change from baseline in (B) βarr2 WT or (D) KO neurons. N= 5, 5 or 6 for untreated, *in vitro* morphine-treated or *in vivo* morphine-

treated βarr2 WT neurons. N=9, 5 or 6 for untreated, *in vitro* or *in vivo* morphine-treated βarr2 KO neurons. All points are mean ± SEM and filled points represent significance from '0' minutes (P<0.05 by two-way repeated-measures ANOVA with Dunnett's post-test). (E) $V_{thresh}$ change across genotypes. N= 7 (untreated), 6 (*in vitro* morphine-treated) and 6 (*in vivo* morphine-treated) in βarr2 WT, and N= 8 (untreated), 6 (*in vitro* morphine-treated) and 6 (*in vivo* morphine-treated) in βarr2 KO groups. Line and error are mean ± SEM. Scatter represents individual data points. *P<0.05, **P<0.01 and 'ns' (not significant, P>0.05) by ordinary two-way ANOVA with Tukey's post-test. 3 µM morphine increased threshold potential in naïve βarr2 WT and KO neurons in a time-dependent manner. The shift in threshold potential was abolished when cells were pre-treated with morphine *in vitro* or *in vivo* irrespective of genotype.

| | | βarr2 WT<br>Ileum myenteric plexus neurons | | | βarr2 KO<br>Ileum myenteric plexus neurons | | |
|---|---|---|---|---|---|---|---|
| | | **Untreated** | ***In vitro* morphine-treated** | ***In vivo* morphine-treated** | **Untreated** | ***In vitro* morphine-treated** | ***In vivo* morphine-treated** |
| **$V_{rest}$ (mV)** | **Baseline** | -45.1 ± 3.0 | -45.4 ± 1.9 | -57.5 ± 2.2 | -52.7 ± 2.5 | -54.4 ± 4.5 | -51.5 ± 2.6 |
| | **+ 3 µM morphine** | -45.3 ± 3.3 | -49.7 ± 0.8 | -55.7 ± 1.8 | -53.4 ± 3.9 | -53.7 ± 4.5 | -51.8 ± 4.1 |
| **$V_{thresh}$ (mV)** | **Baseline** | -20.8 ± 3.8 | -21.9 ± 1.6 | -25.1 ± 1.8 | -25.0 ± 1.5 | -22.1 ± 2.1 | -22.4 ± 2.0 |
| | **+ 3 µM morphine** | -15.3 ± 4.3**** | -23.1 ± 0.9 | -26.4 ± 1.7 | -19.5 ± 1.7**** | -23.6 ± 2.6 | -21.5 ± 2.6 |

**Table 2. Active and passive cellular properties of ileum myenteric plexus neurons from male βarr2 WT and KO mice.** Active and passive properties such as $V_{thresh}$ and $V_{rest}$, respectively, were compared at baseline and after 3 µM morphine. ****P<0.0001 vs. respective baseline of same genotype by repeated-measures two-way ANOVA with Sidak's post-test.

162 **Depletion of β-arrestin-2 does not alter the rate of morphine tolerance to small intestinal motility**

163 We next sought to investigate whether β-arrestin-2 alters the rate at which tolerance develops to
164 morphine-induced inhibition of motility in the small intestine. Furthermore, we also tested sex
165 differences on morphine tolerance. For this purpose, we monitored the time course of the development
166 of morphine tolerance in the small intestine of male (Fig. 4; Table S1) and female (Fig. 5; Table S1) βarr2
167 KO mice. Tolerance was induced by subcutaneously implanting male mice with two 25 mg (denoted as
168 50 mg) morphine pellets or female mice with one 25 mg morphine pellet as these treatment regimens
169 produced significant morphine tolerance in the warm-water tail-withdrawal assay (Fig. 1). The
170 development of tolerance was assessed on indicated days by challenging mice with 10 mg/kg morphine
171 s.c. Charcoal transit through the small intestine was used as a functional metric of motility in the small
172 intestine. Inability of the morphine challenge dose to delay charcoal transit was described as tolerance.

173 An acute 10 mg/kg morphine injection produced robust inhibition of small intestinal transit in all cohorts
174 of male placebo-pelleted mice, evidenced by the reduced charcoal transit (Fig. 4). Exposure to the
175 morphine pellet for one day was sufficient to induce tolerance in the small intestine of male βarr2 WT
176 mice, since charcoal traveled a significantly greater distance in 1-day morphine-pelleted βarr2 WT mice
177 compared to placebo despite 10 mg/kg morphine challenge (1-day PP WT:17.8 ±2.1 % vs. 1-day MP WT:
178 46.7 ±9.1 %; Fig. 4A). Depletion of βarr2 did not delay the expression of small intestinal tolerance as 10
179 mg/kg morphine did not attenuate charcoal transit in 1-day morphine-pelleted βarr2 KO male mice to
180 the same extent as placebo (1-day PP KO: 19.0 ±2.1 % vs. 1-day MP KO: 49.8 ±7.7 %; Fig. 4A; Table S1).
181 Furthermore, the distance traversed by charcoal through the small intestine of 1-day morphine-pelleted
182 WT and KO male mice was comparable (Fig. 4A). This trend was observed in 3, 4 and 7-day morphine-
183 pelleted male WT and KO mice, suggesting that β-arrestin-2 is not required for the development of
184 morphine tolerance in the small intestine of male mice (Figs. 4B, 4C and 4D; Table S1).

185 Similar to the effects in male mice, 10 mg/kg morphine significantly inhibited charcoal transit in placebo-
186 pelleted female mice with or without β-arrestin-2 (Fig. 5). Charcoal transit was greater in 1-day
187 morphine-pelleted female mice compared to the respective placebo controls irrespective of genotype,
188 indicating the development of morphine tolerance (1-day PP WT: 13.0 ±1.2 % vs. 1-day MP WT: 39.5 ±
189 5.2 %, 1-day PP KO: 13.1 ±1.3 % vs. 1-day MP KO: 58.3 ±5.7 %; Fig. 5A; Table S1). Surprisingly, unlike in
190 male mice, there was a significant difference in the distance traveled by charcoal between 1-day
191 morphine-pelleted WT and KO female mice (Fig. 5A; Table S1). However, by Day 7 no difference in
192 charcoal transit was observed between morphine-pelleted WT and KO cohorts (Fig. 5B; Table S1).

193 In conclusion, these results suggest that β-arrestin-2 does not contribute to the development of
194 morphine tolerance in circuits that regulate small intestinal motility of either male or female mice.

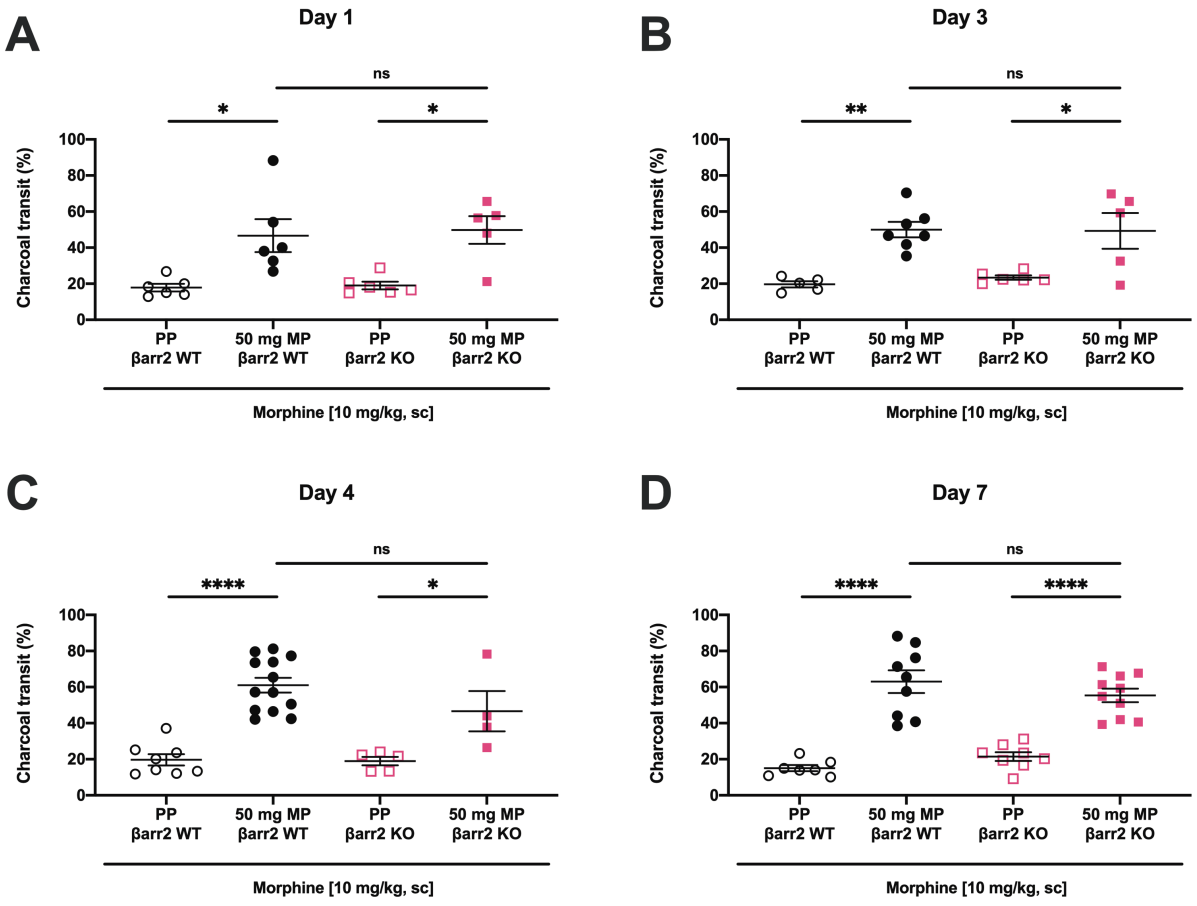


**Figure 4. Morphine tolerance to small intestinal dysmotility in male mice is not mediated by β-arrestin-2.** Morphine tolerance in the small intestine was evaluated using the charcoal transit assay in male βarr2 WT and KO mice pelleted with placebo (PP) or 50 mg (2 x 25 mg) morphine (MP) pellets. Tolerance was assessed day-wise by challenging with 10 mg/kg morphine s.c. on indicated days. Scatter represents individual animals. Line and error are mean ± SEM. *P<0.05, **P<0.01, ****P<0.0001 and ns (not significant, P>0.05) by ordinary two-way ANOVA with Tukey's post hoc test. Morphine tolerance was observed on Day 1 post pelleting. β-arrestin-2 knock out did not alter the rapid development of tolerance.

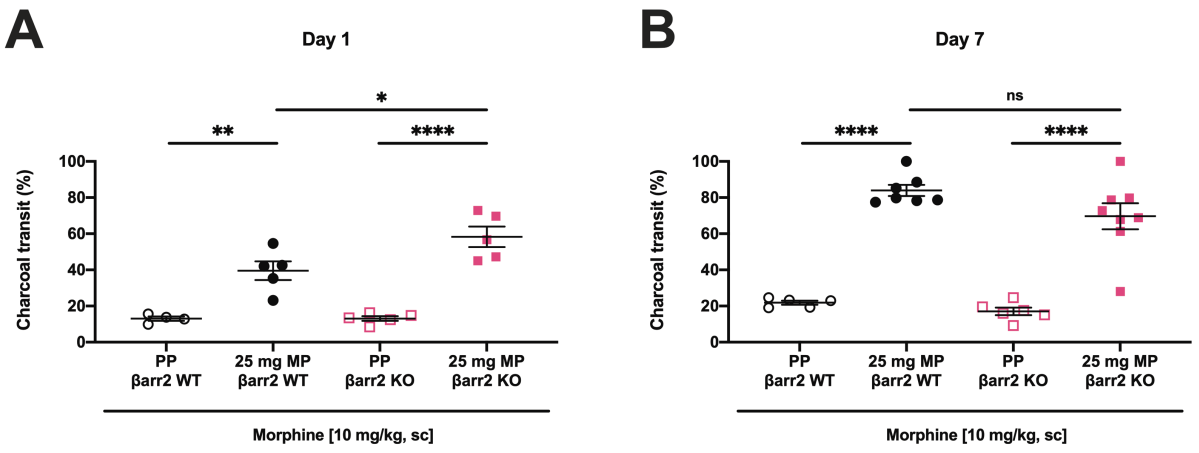


**Figure 5. Morphine tolerance to small intestinal dysmotility in female mice does not require β-arrestin-2.** Morphine tolerance was evaluated using the charcoal transit assay in female βarr2 WT and KO mice pelleted with placebo (PP) or 25 mg morphine (MP) pellet. Tolerance was assessed day-wise by challenging with 10 mg/kg morphine s.c. on indicated days. Scatter represents individual animals. Line and error are mean ± SEM. *P<0.05, **P<0.01, ****P<0.0001 and ns (not significant, P>0.05) by ordinary two-way ANOVA with Tukey's post hoc test. Morphine tolerance in the small intestine was not altered by β-arrestin-2 knock out.

195 **Acute PKC inhibition abrogates *in vivo* morphine tolerance to small intestinal motility**

196 It has been suggested that low-efficacy agonists such as morphine desensitize the MOR and induce
197 tolerance through a PKC-dependent phosphorylation mechanism (Williams *et al.*, 2013). Since morphine
198 tolerance to small intestinal motility is not mediated by β-arrestin-2, we sought to investigate whether
199 PKC mediates morphine tolerance to small intestinal transit *in vivo* using the charcoal transit assay (Fig.
200 6A).

201 7-day 75 mg morphine- or placebo-pelleted male SW mice were injected with 0.6 mg/kg tamoxifen i.p.
202 or vehicle, following which they were challenged with 10 mg/kg morphine s.c. to determine tolerance.
203 10 mg/kg morphine reduced motility in both placebo-pelleted cohorts, as evidenced by the reduced
204 charcoal transit. Vehicle-injected morphine-pelleted mice were resistant to 10 mg/kg morphine-induced
205 inhibition of charcoal transit ($P<0.0001$ versus PP + vehicle), thus implicating tolerance. Alternately, 10
206 mg/kg morphine significantly reduced charcoal transit in morphine-pelleted mice injected with 0.6
207 mg/kg tamoxifen ($P<0.0001$ versus MP + vehicle; Table S1), indicating that morphine tolerance was
208 reversed by PKC inhibition. However, charcoal transit observed in these mice was greater than placebo-
209 pelleted mice acutely challenged with 10 mg/kg morphine ($P<0.01$ versus PP + tamoxifen and $P<0.0001$
210 versus PP + vehicle), which suggested that the reversal of morphine tolerance in the small intestine
211 might be incomplete.

212 In summary, these data show that PKC mediates, at least in part, the development of morphine
213 tolerance in mechanisms that regulate small intestinal motility.

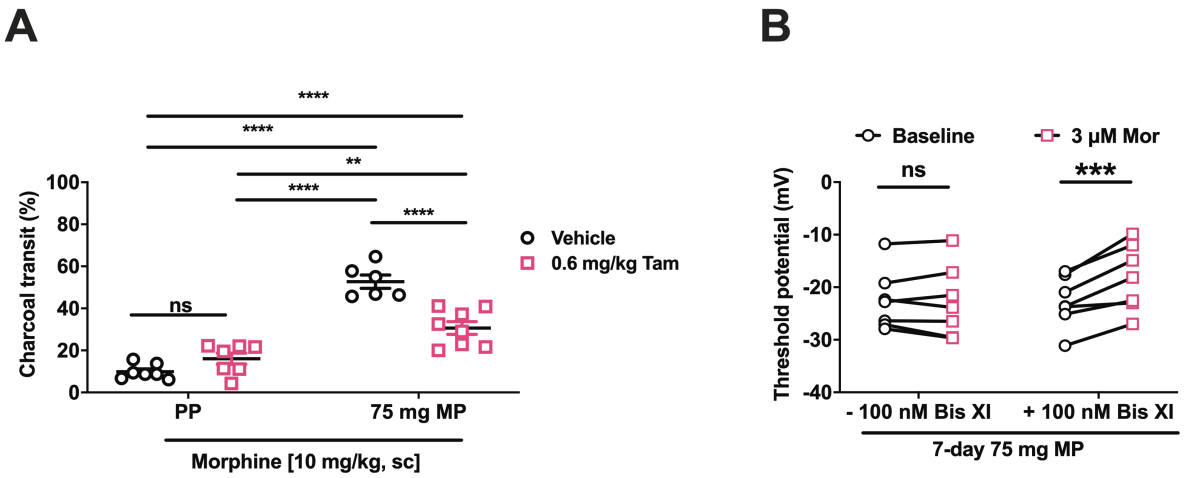


**Figure 6. Morphine tolerance in the small intestine is reversed by acute inhibition of PKC.** (A) Charcoal transit in the presence of 10 mg/kg morphine was measured after acutely injecting 75 mg MP or PP male SW mice with 0.6 mg/kg tamoxifen or vehicle. 0.6 mg/kg tamoxifen partially restored the inhibitory effect of 10 mg/kg morphine in the small intestine of 7-day 75 mg MP male SW mice. Line and error are mean ± SEM. Scatter represents individual animals. N=7 in PP +Vehicle and PP + Tamoxifen; 6 in 75 mg MP + vehicle; and 8 in 75 mg MP + Tamoxifen. **P<0.01, ***P<0.001, ****P<0.0001 and 'ns' (not significant, P>0.05) by two-way ANOVA with Tukey's post-test. (B) Threshold potential at baseline and after 3 μM morphine in individual ileum myenteric plexus neurons isolated from 7-day 75 mg MP male SW mice. Neurons acutely co-treated with 100 nM Bis XI in the pipette solution exhibited morphine-induced depolarization of threshold potential, whereas cells not exposed to Bis XI failed to respond to acute morphine. ***P<0.001 and 'ns' (not significant, P>0.05) by repeated-measures two-way ANOVA with Sidak's post hoc test. N=7/group.

214 **PKC inhibition reverses morphine tolerance in the isolated ileum myenteric plexus neurons**

215 We next investigated if morphine tolerance in the isolated ileum myenteric plexus neurons could be
216 reversed by acute PKC inhibition (Fig. 6B). Similar to earlier electrophysiology experiments, action
217 potential threshold was used as the primary measure of neuronal excitability, such that an increase in
218 threshold potential signified decreased cellular excitability. Ileum myenteric plexus neurons were
219 isolated from male SW mice pelleted with 75 mg morphine for 7 days: a paradigm that produced *in vivo*
220 morphine tolerance in the small intestine (Fig. 6A). Cellular tolerance was determined by measuring
221 threshold potential change in response to acute 3 µM morphine challenge. No significant shift in
222 threshold potential from baseline in response to the morphine challenge dose was described as cellular
223 tolerance.

224 In whole-cell current clamp electrophysiology experiments, threshold potential of *in vivo* chronic
225 morphine-treated ileum neurons did not change when exposed to the acute morphine challenge
226 ($V_{thresh}$: -22.5 ± 2.1 mV to -22.8 ± 2.6 mV; Table 3), implicating cellular tolerance (Fig. 6B). No change in
227 resting potential was detected for baseline versus 3 µM morphine challenge ($V_{rest}$: -51.5 ± 2.8 mV to –
228 51.2 ± -2.8 mV; Table 3). When neurons exposed to chronic morphine *in vivo* and 100 nM Bis XI, a PKC
229 inhibitor, in the internal patch pipette solution were acutely challenged with 3 µM morphine, threshold
230 potential depolarized and morphine tolerance was abolished ($V_{thresh}$: -22.7 ± 1.8 mV to -18.2 ± 2.4 mV;
231 Fig. 6B; Tables 3 and S1). Morphine also decreased the height of the action potential of Bis XI- treated
232 cells (Table 3). Interestingly, resting membrane potential depolarized in these cells ($V_{rest}$: -52.1 ± 3.2 mV
233 to -47.5 ± 2.8 mV; Table 3). However, input resistance, which is a measure of the activity of ion channels
234 at rest, remained unchanged by morphine (Table 3).

235 These results implicate a PKC-mediated cascade, not coupled to β-arrestin-2 downstream, in the

236 neuronal mechanism of morphine tolerance in the small intestine.

| | | - 100 nM Bis XI | + 100 nM Bis XI |
|---|---|---|---|
| $V_{rest}$ (mV) | Baseline | -51.5 ± 2.8 | -52.1 ± 3.2 |
| | + 3 µM morphine | -51.2 ± 2.8 | -47.5 ± 2.8*** |
| $R_{input}$ (MΩ) | Baseline | 621.1 ± 60.0 | 428.4 ± 74.3 |
| | + 3 µM morphine | 582.1 ± 61.6 | 477.0 ± 93.1 |
| $V_{thresh}$ (mV) | Baseline | -22.5 ± 2.1 | -22.7 ± 1.8 |
| | + 3 µM morphine | -22.8 ± 2.6 | -18.2 ± 2.4*** |
| AP height from $V_{rest}$ (mV) | Baseline | 98.8 ± 5.7 | 102.6 ± 5.5 |
| | + 3 µM morphine | 95.9 ± 7.0 | 88.1 ± 9.3* |

**Table 3. Active and passive cellular properties of ileum myenteric plexus neurons from 7-day 75 mg morphine-pelleted male SW mice.** Active properties such as $V_{thresh}$ and action potential height, and passive properties such as $V_{rest}$ and input resistance ($R_{input}$) were compared at baseline and after 3 µM morphine. *P<0.05 and ***P<0.001 vs. respective baseline from the same genotype by repeated-measures two-way ANOVA with Sidak's post-test.

237 **Morphine tolerance develops to small intestinal transit before antinociceptive tolerance**

238 We next sought to determine whether there was a difference in the time course of tolerance
239 development between morphine-induced small intestinal transit and antinociception. Tolerance to the
240 inhibition of motility in the small intestine and antinociception were assessed in same male SW mice
241 subcutaneously implanted with two 25 mg (denoted as 50 mg) morphine pellets for 3 days. As expected,
242 morphine-pelleted mice exhibited maximal baseline tail-withdrawal latency one day after pellet
243 implantation (Fig. 7A). Tail-withdrawal latency progressively declined to pre-pellet levels by Day 3 (Fig.
244 7A). Morphine tolerance to antinociception was tested on Day 3 by measuring tail-withdrawal response
245 to 10 mg/kg morphine challenge or 10 μL/g saline. Data were presented as percent maximal possible
246 effect (%MPE) in Figure 7B. 10 mg/kg morphine induced similar antinociception in 3-day MP and
247 placebo-pelleted mice, indicating that antinociceptive tolerance had not developed in these mice (Fig.
248 7B).

249 In the charcoal transit assay of small intestinal motility, 10 mg/kg morphine significantly attenuated
250 gastrointestinal transit in PP mice from 83.25 ±3.31 % (PP + saline) to 12.64 ±2.28 % (PP + morphine;
251 $P<0.0001$; Fig. 7C; Table S1). However, charcoal transit in mice exposed to morphine pellet for 3 days
252 was not inhibited by the acute challenge (33.98 ±3.91 % in MP + saline versus 33.82 ±1.51 % in MP +
253 morphine; $P>0.05$), indicating that tolerance had developed to morphine- induced inhibition of small
254 intestinal transit (Fig. 7C, Table S1).

255 Collectively, these data show that morphine tolerance in the small intestine occurs before
256 antinociceptive tolerance.

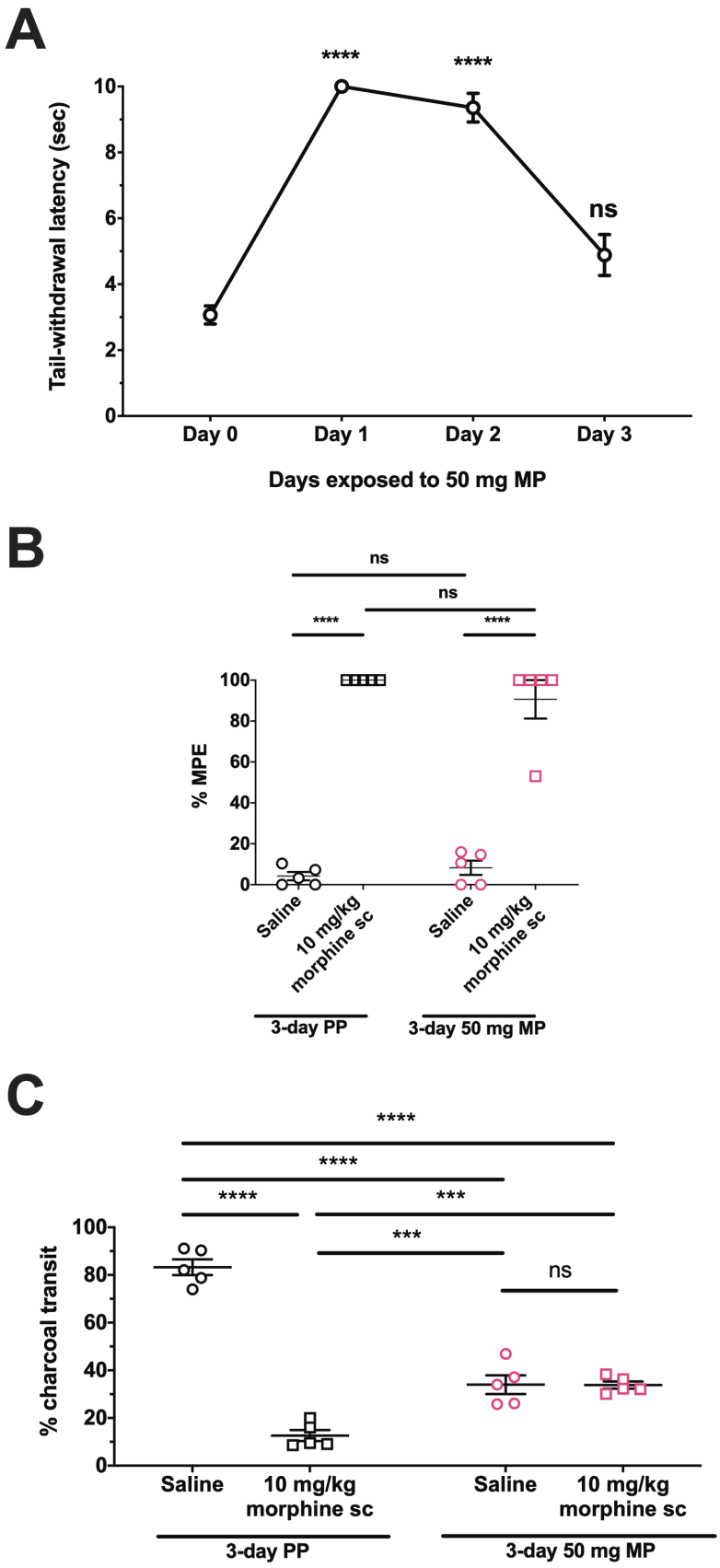
A
****
****
ns
Tail-withdrawal latency (sec)
10
8
6
4
2
0
Day 0
Day 1
Day 2
Day 3
Days exposed to 50 mg MP
B
ns
ns
****
****
% MPE
100
80
60
40
20
0
Saline
10 mg/kg morphine sc
Saline
10 mg/kg morphine sc
3-day PP
3-day 50 mg MP
C
****
****
****
***
***
ns
% charcoal transit
100
80
60
40
20
0
Saline
10 mg/kg morphine sc
Saline
10 mg/kg morphine sc
3-day PP
3-day 50 mg MP

**Figure 7. Morphine tolerance in the small intestine precedes antinociceptive tolerance.** (A) Daily baseline warm-water tail-withdrawal latency in male SW mice pelleted with 50 mg morphine pellet for 3 days. N=9/day; ****P<0.0001 and 'ns' (not significant, P>0.05) versus 'Day 0' by one-way repeated-measures ANOVA with Dunnett's post hoc test. (B) Warm-water tail-withdrawal antinociception reported as percent maximum possible effect (%MPE) in 3-day 50 mg MP or PP male SW mice challenged with 10 mg/kg morphine s.c. or 10 µL/g saline s.c. 3-day MP mice responded to acute morphine in the tail-withdrawal assay, indicating no tolerance. (C) Distance traveled by charcoal through the small intestine, reported as % charcoal transit, in 3-day 50 mg MP or PP male SW mice challenged with 10 mg/kg morphine s.c. or 10 µL/g saline s.c. 3-day MP mice failed to respond to the acute challenge, indicating tolerance. (B, C) N=5/group; ***P<0.001, ****P<0.0001 and 'ns' (not significant, P>0.05) by two-way ANOVA with Tukey's post hoc test. Data are mean ± SEM. Scatter points are individual animals.

257 **Opioid tolerance to GI transit and antinociception**

258 Finally, we compared the rates at which antinociceptive tolerance developed versus opioid induced
259 constipation in male SW mice (Fig. 8). Note that the motility studies described here were capped at 300
260 minutes. Similar to what was previously published, we observed that the mice exhibited antinociceptive
261 behavior in the warm-water tail-withdrawal assay on days 1 and 2 ($P<0.0001$), but showed tolerance to
262 morphine's antinociceptive effects as early as three days following subcutaneous implantation of a 75
263 mg morphine pellet (Fig. 8A). In contrast, these same mice did not show any improvement in GI motility
264 rates until day 5 (240 ± 21.9 min), with significant constipation observed through day 7 compared to
265 placebo controls ($P < 0.001$) as assessed by the carmine dye assay (Fig. 8B). Even though GI motility rates
266 improved significantly on day 7 (200 ± 28.7 min) relative to day 1 (360 ± 0.0 min; $P < 0.0001$), there was
267 clearly a sustained inhibitory effect of morphine that produced prolonged constipation, despite the
268 development of tolerance to opioids and opioid effects elicited elsewhere in the body. This suggests that
269 the prolonged constipation due to opioids might be a result of the lack of tolerance in the colon.

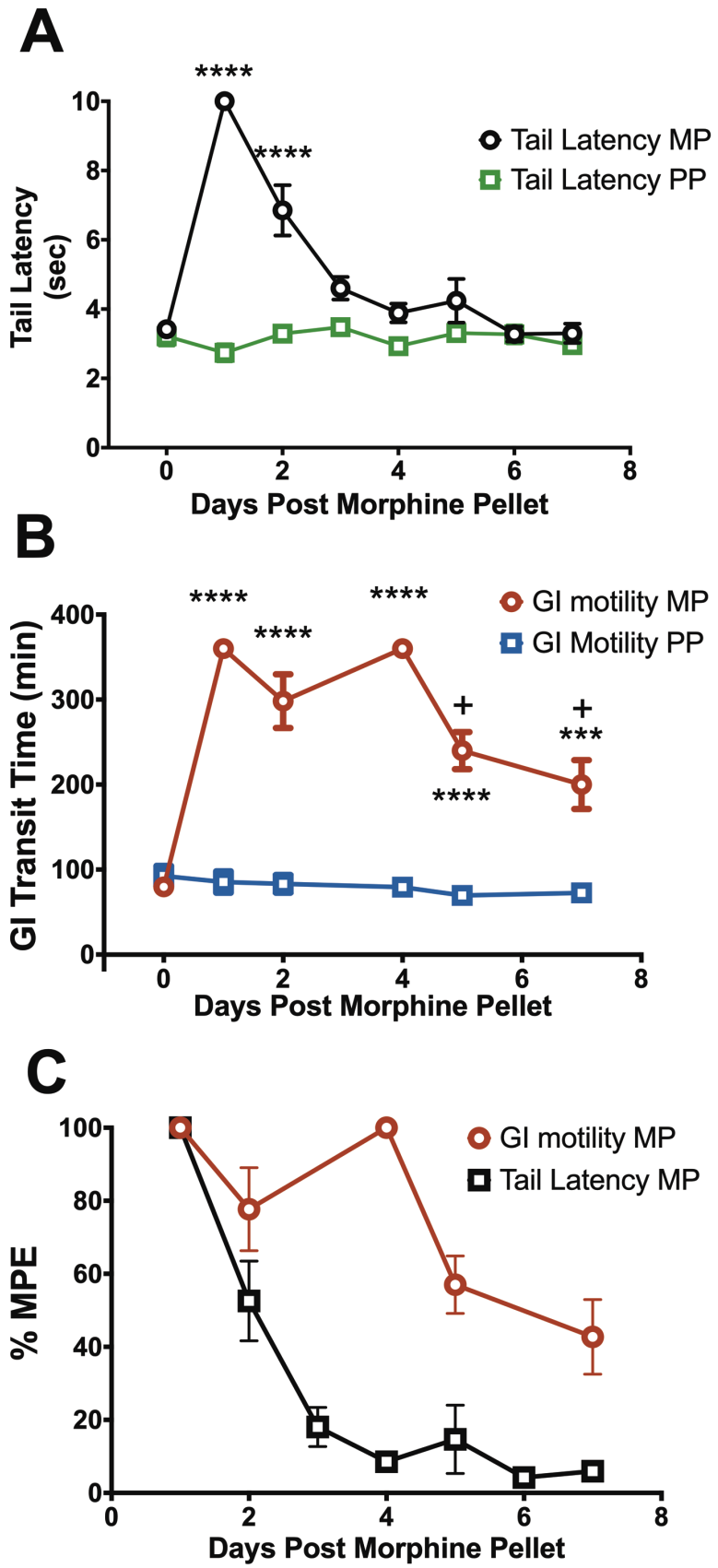
A
****
****
Tail Latency MP
Tail Latency PP
Tail Latency (sec)
Days Post Morphine Pellet
B
****
****
****
****
+
+
***
GI motility MP
GI Motility PP
GI Transit Time (min)
Days Post Morphine Pellet
C
GI motility MP
Tail Latency MP
% MPE
Days Post Morphine Pellet

**Figure 8. Development of Tolerance to Morphine's Antinociceptive and Constipating Effects.** Baseline measures for tail-withdrawal latency at 52°C and total gut motility using oral carmine red dye were taken prior to implantation of a 75 mg morphine pellet (MP) (N = 10) or placebo pellet (PP) (N = 10). Antinociception was assessed daily using the warm-water tail-withdrawal test, beginning 24 hours post MP implantation at 52°C (black) and ending on day 7. In the same animals, total gut motility was assessed as the time (in min) required to pass a fresh red pellet on days 1, 2, 3, 5 and 7. A) Antinociception was observed on days 1 and 2 following MP implantation compared to placebo controls (****P<0.0001). Tolerance to the antinociceptive effects following MP implantation developed rapidly, with no measurable morphine effect following day 3. Data shown are average tail latencies ± SEM, and were analyzed by two-way repeated measures ANOVA with Sidak's post hoc. B) Gut motility was inhibited compared to baseline and placebo measures across all test days (***P<0.001; ****P<0.0001 vs. placebo), with partial tolerance developing following day 5 (+ P< 0.0001 vs. Day 1 MP). Data shown are mean total transit time ± SEM, and analyzed by two-way repeated measures ANOVA with Sidak's post hoc. C) Comparison of rate of tolerance development between GI motility and antinociception in the same animals. Data are expressed as a percent maximum possible effect (%MPE) and represent mean ± SEM, with N = 10.

## Discussion

Traditional opioid agonists have a long-standing history as the most effective compounds for pain relief, however a multitude of side effects complicate their safety margins. Additionally, we know these margins become tighter and the intensity of untoward effects and risk for overdose increase as tolerance develops to the desired analgesic effect. The development of biased opioid agonists that preferentially activate G-protein signaling pathways have generated enthusiasm within the field and new opportunities for treatment of pain with reduced risks (Madariaga-Mazón *et al.*, 2017; Siuda *et al.*, 2017). While there may be promise for some biased opioid agonists, we should be cautious to assume that an improvement in one opioid-dependent measurement equates to an overall improvement compared to the currently approved and clinically-available opioid agonists.

Using the β-arrestin-2 knock out transgenic mouse model as a tool, the present study demonstrated that morphine tolerance in ileum myenteric plexus neurons and to small intestinal transit develops rapidly and independently of the β-arrestin-2 desensitization pathway in both male and female mice. Moreover, morphine tolerance in neurons and to small intestinal transit is reversed by acute inhibition of PKC, suggesting that in the ileum tolerance is mediated by PKC phosphorylation. The results also show that tolerance to the same ligand—morphine—develops at a faster rate to small intestinal motility compared to spinally-mediated antinociception, tolerance to which manifests before whole GI transit. This indicates that the chronic constipation due to long-term opioid use might be a colonic effect. Taken together, the findings presented in the current study implicate that tolerance in the small intestine may develop even if the β-arrestin-2 pathway is attenuated, for example by using biased agonists such as Oliceridine, which recently completed Phase 3 clinical trials (Hertz, 2018; Bergese *et al.*, 2019). Mechanisms of tolerance and dependence are closely related and tolerance is often considered as a gateway to the development of physical dependence of which diarrhea is a common symptom (Wesson

293 and Ling, 2003; Donroe *et al.*, 2016). Withdrawal-induced diarrhea could be due to the development of
294 tolerance in the ileum as opioid tolerance does not develop in the colon (Ross *et al.*, 2008; Kang *et al.*,
295 2012; Maguma *et al.*, 2012). Indeed, several studies have previously reported the precipitation of
296 spontaneous and naloxone-induced withdrawal in the isolated ileum of rodents (Collier *et al.*, 1981;
297 Warhurst *et al.*, 1984; Bianchetti *et al.*, 1986; Johnson *et al.*, 1987). In addition, we have previously
298 demonstrated that naloxone induces hyperexcitability in myenteric plexus neurons of the ileum but not
299 the colon of chronic morphine-treated mice (Smith *et al.*, 2014). Furthermore, Naldemedine, a
300 peripherally-acting MOR antagonist clinically used to mitigate opioid-induced constipation in chronic
301 pain patients, is known to commonly cause diarrhea, sometimes severe enough to result in drug
302 discontinuation (Katakami *et al.*, 2017, 2018). Given the findings presented here and in a previous study
303 that reported intact diarrhea in morphine-withdrawn β-arrestin-2 knock out mice (Bohn *et al.*, 2000), it
304 is likely that biased agonists induce dependence in the small intestine even if antinociceptive tolerance
305 is mitigated. Consequently, the findings presented here raise questions about the usefulness of G
306 protein-biased agonists to circumvent adverse effects associated with traditional opioid use.

307 MOR desensitization is considered as the first step leading to tolerance. β-arrestin-2 is a scaffolding
308 protein that is recruited to the MOR and causes uncoupling of the receptor from G-proteins, leading to
309 MOR desensitization (Williams *et al.*, 2013). This desensitization pathway is widely believed to be the
310 basis of opioid tolerance, specifically antinociceptive tolerance (Bohn *et al.*, 2000). However, in the
311 present study we observed that morphine tolerance to small intestinal transit *in vivo* is not mediated by
312 β-arrestin-2. This finding is in line with previous studies reported by our laboratory that attenuation of
313 β-arrestin-2 by genetic deletion or use of biased agonists such as TRV130 (Oliceridine) produce tolerance
314 in the isolated ileum tissue (Kang *et al.*, 2012; Altarifi *et al.*, 2017).

315 Opioids are known to increase sphincter tone and delay gastric emptying (Bayguinov and Sanders, 1993;
316 Holzer, 2009) and the kinetics of tolerance to this effect could be different. This might explain why
317 transit through the small intestine is reduced in some experiments and the perceived lack of complete
318 tolerance in the small intestine of tolerant animals.

319 Motility in the gastrointestinal tract is a combination of coordinated neurogenic and myogenic functions
320 (Costa, 2000). Therefore, mechanisms mediating morphine tolerance in isolated tissues or to small
321 intestinal motility in intact animal might not represent mechanisms underlying tolerance in neurons. The
322 ileum myenteric plexus contains cell bodies of neurons innervating the longitudinal and circular smooth
323 muscles of the gut wall. They coordinate peristaltic contractions in the ileum (Furness *et al.*, 2014). Here,
324 we found that morphine tolerance in isolated myenteric neurons is not mediated by β-arrestin-2. Both,
325 "acute" and "long-term" tolerance were not altered by β-arrestin-2 deletion in neurons (as defined by
326 Williams *et al.*, 2013). These results correlated with findings at the whole-animal level. Altogether, these
327 results indicate conclusively that opioid tolerance in the small intestine is not regulated by β-arrestin-2
328 desensitization at the level of intact animals, isolated tissues and single neurons.

329 MOR regulation is strongly agonist dependent (Williams *et al.*, 2013). High-efficacy agonists such as
330 DAMGO are known to strongly recruit β-arrestin-2 to internalize the MOR, whereas low-efficacy agonists
331 such as morphine do not readily internalize the MOR. In the present study, we used only morphine—a
332 clinically-approved analgesic and active metabolite of heroin—to demonstrate that opioid tolerance in
333 the small intestine is β-arrestin-2-independent. However, we have previously also shown that tolerance
334 in the isolated ileum tissue develops to repeated administration of high efficacy opioids like DAMGO,
335 fentanyl and etorphine (Maguma *et al.*, 2012). Consequently, the β-arrestin-2-independent mechanism
336 of tolerance in the ileum is not contingent on the opioid agonist.

337 The intracellular kinase involved in MOR phosphorylation and subsequent desensitization is agonist-
338 selective and morphine, in particular, is known to preferentially induce PKC phosphorylation of the MOR
339 (Bailey *et al.*, 2006; Williams *et al.*, 2013). MOR phosphorylation, including by PKC, has been implicated
340 in the mechanism of *in vivo* tolerance to antinociception (Smith *et al.*, 1999, 2003, 2006; Inoue and
341 Ueda, 2000; Bohn *et al.*, 2002; Hua *et al.*, 2002; Gabra *et al.*, 2008; Kliewer *et al.*, 2019) and cellular
342 tolerance in DRG neurons (Jacob *et al.*, 2018) and locus coeruleus neurons (Levitt and Williams, 2012;
343 Arttamangkul *et al.*, 2018). Interestingly, PKC also mediates morphine tolerance to small intestinal
344 transit *in vivo* and in isolated myenteric plexus neurons as evidenced by the findings presented here.
345 These findings are supported by observations previously reported by Wang et al., who found that PKC
346 mediated tolerance to sufentanil-induced reduction of cAMP production in chronic morphine-treated
347 guinea pig ileum (Wang *et al.*, 1996). PKC is a promiscuous molecule and can cause homologous and
348 heterologous desensitization of downstream pathways or ion channels (Gold *et al.*, 1996; Dang and
349 Christie, 2012; Levitt and Williams, 2012). A previous study reported that PKC inhibition reduced the
350 conductance of voltage-gated sodium channels, which are pivotal in the generation of action potentials
351 (Gold *et al.*, 1996; Ma *et al.*, 2019). However, we did not observe any change in action potentials evoked
352 by chronic morphine-treated ileum neurons treated with or without the PKC inhibitor, Bis XI.
353 Alternately, co-treatment of Bis XI with morphine altered neuronal excitability and implicated reversal of
354 morphine tolerance. This indicated that morphine tolerance in ileum neurons due to PKC
355 phosphorylation might be MOR-mediated and not a direct effect on the ion channel. This is supported
356 by findings that, heterologous desensitization of the noradrenergic pathway was not observed in
357 tolerant locus coeruleus neurons, which utilize the PKC phosphorylation for tolerance development
358 (Levitt and Williams, 2012).

359 Previous studies have reported highly variable sex differences in opioid-induced analgesia in both
360 humans and rodents that are subject to the type of agonist (humans and rodents), pain model (humans

361 and rodents), study design (humans), genotype (rodents), species (rodents), route of administration
362 (rodents), and supplier of animals (Bodnar and Kest, 2010; Lee and Ho, 2013). While we did not observe
363 sex differences in the potency of acute morphine, differences were observed in the effects of chronic
364 morphine. In the present study, we found that a smaller dose of morphine was required to induce
365 tolerance in wild-type female mice compared to male mice. This could be due to the differential
366 influence of sex hormones on pathways mediating morphine tolerance. Indeed, a previous study has
367 demonstrated that ovariectomized rats are refractory to morphine tolerance, indicating that estrogen
368 might be an important mediator of opioid tolerance in female rats (Shekunova and Bespalov, 2004,
369 2006). While sex hormones have been noted previously to influence gastrointestinal physiology (Pines *et*
370 *al.*, 1998; Afonso-Pereira *et al.*, 2018), no differences were noted in the rate of morphine tolerance or in
371 the role of β-arrestin-2 in the development of morphine tolerance to small intestinal motility between
372 male and female mice.

373 Opioid tolerance in different tissues is known to develop at different rates (Ling *et al.*, 1989; Hayhurst
374 and Durieux, 2016). In this study, we use the same ligand—morphine—to show that tolerance to small
375 intestinal transit develops before antinociceptive tolerance. Morphine tolerance to whole GI transit is
376 incomplete and the slowest to develop, suggesting that chronic constipation could be a function of lack
377 of tolerance in the colon. The findings presented here suggest that the underlying mechanisms for the
378 differences in the rates and extent of tolerances to the same ligand result from different cellular
379 pathways employed by the MOR. We found that morphine tolerance in the ileum myenteric plexus,
380 which regulates intestinal motility, and to small intestinal transit develops via a PKC-mediated
381 mechanism independent of β-arrestin-2. In contrast, antinociceptive tolerance is purportedly mediated
382 by β-arrestin-2, whereas tolerance in the colon is inhibited by β-arrestin-2 (Bohn *et al.*, 2000; Kang *et al.*,
383 2012). Nociceptive DRG neurons are the first-order neurons of ascending and reflexive pain pathways
384 and have been previously implicated in the expression of opioid-induced antinociception and induction

385 of tolerance (Chen *et al.*, 2007; Corder *et al.*, 2017; Sun *et al.*, 2019). Analysis of single-cell RNA
386 sequencing data from Zeisel at al. (Zeisel *et al.*, 2018) and Usoskin et al. (Usoskin *et al.*, 2015) revealed
387 differential expression of *Scna10a*, which encodes for Nav1.8, in DRG neurons and ileum myenteric
388 neurons that co-express *Oprm1* (gene for MOR; Fig. S3). Nav1.8 is expressed in TRPV1-expressing
389 nociceptive DRG neurons but not myenteric neurons from the ileum. On the other hand, Nav1.7 is
390 expressed in both ileum and DRG neurons. Voltage-gated sodium channels are critical in the upstroke of
391 the action potential and we and others have demonstrated that acute and chronic morphine exposure
392 alters the activation and inactivation dynamics of these sodium channels in DRG nociceptors and
393 myenteric plexus neurons (Chen *et al.*, 2012; Kang *et al.*, 2012; Smith *et al.*, 2012, 2014; Bardoni *et al.*,
394 2014; Mischel *et al.*, 2018). Thus, the discrete mechanisms of opioid tolerance to various physiological
395 effects could be due to differences in MOR-ion channel coupling at the cellular level.

396 Our conclusions from this series of studies are that in the ileum, tolerance at the MOR is extremely
397 rapid—quicker than antinociceptive tolerance—and is mediated by a PKC-dependent mechanism not
398 involving β-arrestin-2. This is in contrast to the finding that analgesic tolerance is caused by β-arrestin-2
399 (Bohn *et al.*, 2000). This suggests that different rates of morphine tolerances could be due to discrete
400 mechanisms in various systems. Consequently, this complicates the approach of using biased agonists as
401 side effects such as diarrhea and constipation will likely remain with chronic opioid use.

402

403

404

405

406

407 **Materials and Methods**

408 **Drugs and Chemicals**

409 Morphine sulfate pentahydrate was obtained from the National Institutes of Health National
410 Institute on Drug Abuse (Bethesda, MD). Pyrogen-free isotonic saline was purchased from Hospira (Lake
411 Forest, IL). Dulbecco's modified Eagle's medium (DMEM)/F12, Neurobasal-A medium, $Ca^{2+}$ and $Mg^{2+}$-
412 free Hank's balanced salt solution (HBSS), Trypsin-EDTA (0.25%), 50x B-27 supplement and L-glutamine
413 were purchased from Gibco, Thermo Fisher Scientific (Waltham, MA).
414 Penicillin/streptomycin/amphotericin B antibiotic-antimycotic solution and Laminin were purchased
415 from Corning (Corning, NY). Colagenase Type 2 was purchased from Worthington Biochemical
416 Corporation (Lakewood, NJ). Glial cell line-derived neurotrophic factor (GDNF) was purchased from
417 Neuromics (Edina, MN). Poly-D-lysine was purchased from MiliporeSigma (Burlington, MA). Fetal Bovine
418 serum (FBS) and bovine serum albumin (BSA) were purchased from Quality Biological, (Gaithersburg,
419 MD) and American Bioanalytical (Canton, MA) respectively. Glass cover slips were purchased from
420 ThermoFisher Scientific (Waltham, MA). Twenty-four-well culture dishes and 35 x 10 mm petri dishes
421 were purchased from CELLTREAT (Pepperell, MA). $CaCl_2$, $MgCl_2$, NaCl, KCl, HEPES, EGTA, $NaH_2PO_4$,
422 glucose, $Na_2ATP$, NaGTP, L-aspartic acid (K salt), KOH, NaOH, $MgSO_4$, $NaHCO_3$, Bisindolylmaleimide (Bis)
423 XI, charcoal, carmine red dye, tamoxifen, corn oil, and carboxymethylcellulose was purchased from
424 MilliporeSigma (Burlington, MA). Gum arabic was purchased from Acros Organics (Fairlawn, NJ).

425

426 **Animals**

427 Swiss Webster (SW) male mice (Envigo, Indianapolis, IN), male and female β-arrestin-2 (βarr2)
428 knock out (KO) or their wild-type (WT) littermates, and female MOR-mCherry mice (The Jackson

429 Laboratory, Bar Harbor, ME) were separately group housed with up to five animals per cage in animal-
430 care quarters maintained on a 12-hour light/dark cycle. Mice used in experimental procedures were at
431 least 7 weeks of age. Male SW mice weighed 25-35 g, male β-arrestin-2 mice weighed 20-25 g, and
432 female β-arrestin-2 mice weighed 19-23 g. Mice were acclimated in the vivarium for at least one week
433 prior to experimentation. Breeding pairs for the β-arrestin-2 mice were initially obtained from Dr.
434 Lefkowitz (Duke University, Durham, NC) and housed within the transgenic facility at Virginia
435 Commonwealth University. The genetic background of the β-arrestin-2 WT and KO mice used in our
436 experimental procedures was 81% C57B6J:19% C57B6N. MOR-mCherry reporter mice were generously
437 provided by Dr. J. González-Maeso (Virginia Commonwealth University). Mice had access to food and
438 water *ad libitum* unless specified otherwise. All animal care and experimental procedures were
439 conducted in accordance with procedures reviewed and approved by the Institutional Animal Care and
440 Use Committee at Virginia Commonwealth University.
441

442 ***In vivo* morphine treatment**

443 Subcutaneously implanted continuous-release morphine pellets were used to model chronic *in*
444 *vivo* exposure as pellets maintain a high plasma level of morphine over a longer period of time
445 compared to intermittent injections or osmotic pumps and the tolerance induced is more robust (Dighe
446 *et al.*, 2009; McLane *et al.*, 2017). Where indicated, one 75 mg, or one or two 25 mg morphine pellets
447 were implanted subcutaneously in the dorsum of male SW, or male or female β-arrestin-2 KO mice and
448 their WT phenotypes for 7 days. Male SW mice were implanted subcutaneously with two 25 mg
449 morphine pellets for 3 days only in the Figure 7 experiment. The dose of two 25 mg morphine pellets is
450 denoted as "50 mg" throughout the present study. In all experiments, control mice were implanted with
451 one or two placebo pellets. In order to insert the pellet, mice were first anesthetized with 2.5%
452 isoflurane before shaving the hair from the base of the neck. Skin was disinfected with 10% povidone

453 iodine (General Medical Corp, Walnut, CA) and alcohol. A 1 cm horizontal incision was made at the base
454 of the neck and one or two pellets were inserted in the subcutaneous space. The surgical site was closed
455 with Clay Adams Brand, MikRon AutoClip 9-mm wound clips (Becton Dickinson, Franklin Lakes, NJ) and
456 cleansed with 10% povidone iodine. Use of aseptic surgical techniques minimized any potential
457 contamination of the pellet, incision and subcutaneous space. Mice were allowed to recover in their
458 home cages where they remained throughout the experiment.
459

460 **Isolation of myenteric neurons from ileum**

461 Myenteric plexus neurons were isolated from the longitudinal muscle of naïve male β-arrestin-2
462 WT or KO mouse ileum as described by Smith et al., 2013 (Smith *et al.*, 2013). Mice were euthanized by
463 cervical dislocation and the ileum was immediately transferred to cold (4$^{o}$C) Krebs solution (in mmol/L:
464 118 NaCl, 4.6 KCl, 25 $NaHCO_3$, 1.3 $NaH_2PO_4$, 1.2 $MgSO_4$, 11 glucose, 2.5 $CaCl_2$) bubbled with carbogen
465 (95% $O_2$/5% $CO_2$) gas. Intestinal digesta was flushed out with cold Krebs following which the intestine
466 was transferred to a beaker containing clean ice-cold Krebs buffer. The intestine was cut into 2-4 cm
467 segments and each segment was threaded onto a plastic rod. Longitudinal muscle to which the
468 myenteric plexus is attached was gently teased apart with a moist cotton applicator and collected in
469 clean carbogen-bubbled, ice-cold Krebs. Longitudinal muscle pieces were rinsed three times in 1 mL
470 Krebs and collected by centrifugation (350 x g; 30 seconds; 4$^{o}$C). Longitudinal muscle sheets were
471 minced into smaller pieces with a scissor and incubated at 37$^{o}$C for 60 minutes with 1.3mg/mL
472 collagenase type 2 and 0.3 mg/mL BSA in carbogen-bubbled Krebs. Following collagenase digestion,
473 tissue was collected by centrifugation (350 x g; 8 minutes; 4$^{o}$C) and supernatant was discarded. Tissue
474 was then incubated at 37$^{o}$C for 8 minutes in 0.05% trypsin-EDTA in $Ca^{2+}$ and $Mg^{2+}$ -free HBSS. Digestion
475 was halted by neutralizing trypsin with DMEM/F12 media supplemented with 10% FBS. Tissue was
476 filtered through a sterile Nitrex mesh and cells were collected by centrifugation at 350 x g for 8 minutes

477 at 4$^{o}$C. Supernatant was decanted and cells were resuspended in Neurobasal-A media supplemented
478 with 1% FBS, 1x B-27, 10 ng/mL GDNF, 2 mM L-glutamine, and antibiotic-antimycotic solution. Isolated
479 cells were plated on poly-D-lysine and laminin-coated glass coverslips and maintained at 37$^{o}$C in a
480 humidified 5% $CO_2$/air-enriched incubator. 15-18 hours later, cells were used in patch clamp
481 experiments. Where indicated, cells were cultured in media supplemented with morphine sulfate
482 pentahydrate for 15-18 hours (overnight) prior to patch clamp electrophysiology experiments.

483 Cells were also isolated from male β-arrestin-2 WT or KO mice subcutaneously implanted with
484 50 mg morphine pellet for 7 days or male SW mice subcutaneously implanted with 75 mg morphine
485 pellet for 7 days using the procedure described above. Isolated cells were incubated as described above
486 in Neurobasal-A media supplemented with growth factors and antibiotic-antimycotic solution for 15-18
487 hours.

488

489 **Whole-cell patch clamp electrophysiology**

490 Coverslips with adherent cells were transferred to a microscope stage plate continuously
491 superfused with external physiological salt solution composed of 135 mM NaCl, 5.4 mM KCl, 0.33 mM
492 $NaH_2PO_4$, 5 mM HEPES, 5 mM glucose, 2 mM $CaCl_2$ and 1 mM $MgCl_2$, and adjusted to a pH of 7.4 with 1
493 M NaOH. Patch pipettes (2-4 MΩ) made from pulled (Model P-97 Flaming-Brown Micropipette Puller,
494 Sutter Instruments, Novato, CA) and fire-polished borosilicate glass capillaries (World Precision
495 Instruments, Sarasota, FL) were filled with internal physiological solution and used to form a GΩ
496 resistance seal with the cell. The internal physiological solution was composed of 100 mM L-aspartic acid
497 (K salt), 30 mM KCl, 4.5 mM $Na_2ATP$, 1 mM $MgCl_2$, 10 mM HEPES, 0.1 mM EGTA and 0.5 mM NaGTP and
498 pH adjusted to 7.2 with 3 M KOH. 100 nM Bis XI was added to the internal physiological solution in
499 experiments designed to test the effect of PKC inhibition on cellular tolerance. Whole-cell current clamp
500 recordings were made at room temperature using HEKA EPC 10 amplifier (HEKA, Bellmore, NY) at a 10

501 kHz sampling frequency and 2.9 kHz low-pass Bessel filtering. PatchMaster v2x60 (HEKA) was used for
502 pulse generation and data acquisition. All current clamp recordings were performed five minutes after
503 achieving whole-cell mode to allow dialysis of internal solution. Experiments were performed only on
504 cells with healthy morphology and stable patch. Ileum myenteric plexus neurons were held at 0 pA
505 resting current and a 10 pA pulse was applied in 5 pA steps starting from -30 pA to assess passive and
506 active cells properties. Previously, myenteric plexus neurons with after-hyperpolarization (AHP) have
507 been demonstrated to respond to morphine in patch clamp experiments (Smith *et al.*, 2012, 2014).
508 Furthermore, in the present study we observed that MOR-mCherry-positive ileum neurons that
509 responded to morphine in patch clamp experiments exhibited AHP (Fig. S2). Therefore, only ileum
510 myenteric plexus neurons with AHP were tested in experiments.

511 Effect of morphine on excitability of ileum neurons was evaluated by superfusing external
512 physiological solution containing 3 µM morphine and measuring action potential characteristics every
513 two minutes for up to 16 minutes. Active and passive cellular properties such as threshold potential
514 ($V_{thresh}$), action potential spike height, resting membrane potential ($V_{rest}$) and input resistance ($R_{input}$)
515 were compared before and after 3 µM morphine exposure. Action potential threshold was defined as
516 the voltage at which the first derivative of the membrane voltage with respect to time (dV/dt)
517 significantly deviated from zero in the course of an action potential upstroke. It was used as the primary
518 measure of neuronal excitability in our experiments. Cellular tolerance was assessed identically in cells
519 either incubated with 10 µM morphine overnight or isolated from mice implanted with one 75 mg or
520 two 25 mg morphine pellets for 7 days. Values reported were not corrected for junction potentials (~12
521 mV). In all patch clamp experiments, "N" represents the total number of cells within each group from
522 which recordings were obtained. These values represent independent observations and not replicate
523 values. Cells were isolated from at least 3-5 different animals. Where indicated, threshold potential

524 change from baseline values was calculated using the formula: threshold potential change = (Test
525 threshold potential at 16 minutes) – (baseline threshold potential).
526
527 **Behavioral testing**
528 All testing was conducted in a temperature and light-controlled room in the light phase of the
529 12-hour light/dark cycle. Mice were acclimated to the testing room for at least 15-18 hours before
530 commencing experiments to eliminate confound from potential stress-induced effects on
531 antinociception and gastrointestinal motility (Sorge *et al.*, 2014). All animals were randomly divided into
532 control and treatment groups. Mice were excluded from experiments if they exhibited wounds from
533 aggressive interactions with cage mates, since injury-induced activation of the endogenous opioid
534 system could confound nociceptive and gastrointestinal motility assays (Corder *et al.*, 2013).
535 Experimenters were not blinded to the identity of the groups; however, all behavioral testing was
536 performed and repeated by multiple experimenters (K.H.M., J.C.J., I.A., S.H. and A.K) to ensure reliability
537 of results.
538
539 **Charcoal meal transit assay**
540 The charcoal meal transit assay was used to measure gastrointestinal motility through the small
541 intestine. In this assay, mice were fasted for 4-6 hours with *ad libitum* access to water on a wire mesh to
542 prevent consumption of feces and bedding. Fasted mice were injected subcutaneously with either saline
543 (10 µL/g of body weight) or morphine (10 mg/kg) 30 minutes before administering a suspension of 5%
544 aqueous charcoal in 10% gum arabic by oral gavage at dose of 10 µL/g of body weight. 20 minutes later,
545 mice were euthanized by cervical dislocation and the entire small intestine from the jejunum to the
546 cecum was resected. Distance traveled by the leading edge of the charcoal meal was measured as a
547 percentage of the total length of the small intestine and represented as % charcoal transit.

548

549

550

551 **Total Gastrointestinal Transit Assay with Carmine Dye.**

552 Total oral to anal GI transit time was measured using the carmine red dye method as previously
553 described (Kimball *et al.*, 2005; Li *et al.*, 2011). A solution of carmine red, which cannot be absorbed
554 from the lumen of the gut, consisted of 6% (w/v) carmine red dye powder in 0.5% (w/v)
555 carboxymethylcellulose vehicle (in $ddH_20$). Each animal was orally gavaged with 150 µl of the carmine
556 red solution through a 21-gauge round-tipped feeding needle and immediately placed in an empty cage
557 with no bedding. Animals had access to water, but no food, during testing. The time of gavage was
558 recorded as $T_0$. Fecal pellets were monitored in 15-minute intervals for the presence of carmine red in
559 the feces. Total transit time was determined as the interval between $T_0$ and the production of the first
560 fecal pellet fully incorporating the carmine dye. These times are reported as Total Transit Time in
561 minutes. The studies were capped at 300 minutes. Where noted, total GI transit was also normalized
562 within subjects as percent maximum possible effect (%MPE) calculated as: [(Test day transit time-Day 0
563 baseline transit time)/ (300- Day 0 baseline transit time)] x 100, adapted from Harris and Pierson, 1964
564 (Harris and Pierson, 1964).

565

566 **Evaluating thermal nociception**

567 Thermal nociception was examined using the warm-water tail-withdrawal assay. In the warm-
568 water tail-withdrawal assay, mice were gently secured in a cloth and the distal 1/3$^{rd}$ of the tail was
569 immersed in a water bath warmed to 56$^{o}$C $\pm$ 0.1$^{o}$C or 52$^{o}$C $\pm$ 0.1$^{o}$C. The latency to withdraw the tail
570 from the water was recorded. A maximum cut-off of 10 seconds was set to prevent damage to the tail.
571 Only naïve mice with control latency between 2 and 4 seconds were used in experiments. Tolerance was

572 assessed by challenging mice with an acute subcutaneous injection of 10 mg/kg morphine, which was
573 the ~ED80 dose of morphine in male mice. Morphine challenge latency was compared against baseline
574 latency. Where indicated, antinociception was quantified as %MPE, which was calculated as follows:
575 %MPE= [(morphine challenge latency-baseline latency)/ (10-baseline latency)] x 100, adapted from
576 Harris and Pierson, 1964 (Harris and Pierson, 1964).
577

578 **Morphine cumulative dose response curve**

579 Baseline tail-withdrawal latencies were recorded as described above for 7-day placebo or
580 morphine-pelleted (MP) male or female β-arrestin-2 mice. Placebo-pelleted (PP) mice were injected
581 subcutaneously every 30 minutes with 0.5, 0.5, 1, 2, 4 and 8 mg/kg morphine to achieve final cumulative
582 doses of 0.5, 1, 2, 4, 8 and 16 mg/kg morphine. The final cumulative morphine doses evaluated in
583 morphine-pelleted mice were 2, 4, 8, 16, 32, 64 and 128 mg/kg s.c. morphine. Tail-withdrawal latencies
584 were recorded every 30 minutes, following which mice were immediately injected with the next
585 morphine dose. Antinociception was quantified as %MPE as described above.
586

587 **Tamoxifen reversal of tolerance**

588 To assess the role of PKC in the mechanism of morphine tolerance, male SW mice were
589 implanted subcutaneously with one 75 mg morphine or placebo pellet for 7 days. On the test day (Day
590 7), mice were fasted for 4-6 hours on a wire-mesh with *ad libitum* access to water. Subsequently, mice
591 were injected intraperitoneally with 0.6 mg/kg tamoxifen in corn oil or only corn oil. 30 minutes later, 10
592 mg/kg morphine s.c. was injected and an additional 30 minutes later tail-withdrawal latency was re-
593 tested to evaluate antinociception. The tamoxifen treatment protocol was adopted from Withy et al.
594 (Withey *et al.*, 2017). Subsequently, each mouse received an oral gavage of 10 µL/g charcoal meal and
595 20 minutes later charcoal transit was assessed.

596

597

598

599 **RNA isolation and real-time PCR**

600 Quantitative real-time polymerase chain reaction (qRT-PCR) was performed on a Mini-Opticon
601 real-time PCR system (Bio-Rad, Hercules, CA). Ribosomal 18S RNA was used as an internal control. Spinal
602 cord samples were isolated from naïve male β-arrestin-2 WT and KO mice, and TRIzol (Thermo Fisher
603 Scientific, Waltham, MA) was used to extract total RNA according to the manufacturer's protocol. A
604 spectrophotometer (Smart Spec Plus, Bio-Rad, Hercules, CA) was used to determine the concentration
605 and purity of RNA samples. iTaq Universal SYBR Green One-Step Kit (Bio-Rad, Hercules, CA) was used to
606 perform real-time PCR. 200 ng total RNA was added to the reaction mixture. Expression of the β-
607 arrestin-2 gene relative to 18S expression was quantified using the ΔΔCt method and plotted as fold
608 change over 18S expression. Spinal cord samples were obtained from four β-arrestin-2 WT and KO mice
609 each and PCR analysis was duplicated for each sample. Primers utilized in this study were as follows:

| Target gene | Primer sequence |
|---|---|
| **Mouse β-arrestin-2** | Forward: 5'-TCGAGCCCTAACTGCAAG-3' |
| | Reverse: 5'-CCCTGTGGCTTCTTCAGACT-3' |
| **Mouse 18S** | Forward: 5'-TCAAGAACGAAAGTCGGAGG-3' |
| | Reverse: 5'-GGACATCTAAGGGCATCAC-3' |

**Table 1. Primer sequence of mouse β -arrestin-2 and 18S**

610 **Analysis of published single-cell RNA sequencing data of mouse ileum myenteric plexus and dorsal**
611 **root ganglia neurons**

612 Single-cell RNA sequencing data of naïve mouse ileum myenteric neurons and dorsal root
613 ganglia (DRG) neurons published by Zeisel et al. (Zeisel *et al.*, 2018) available at
614 http://mousebrain.org/genesearch.html) and Usoskin et al. (Usoskin *et al.*, 2015); available at
615 http://linnarssonlab.org/drg/), respectively, was analyzed to visualize the expression of indicated genes
616 in heat maps. Ileum neurons were isolated from the myenteric plexus and clustered into ENT 1-9 by
617 Zeisel et al., and DRG neurons from L4-L6 were isolated and clustered into NP (non-peptidergic) 1-3, PEP
618 (peptidergic) 1-2, NF (neurofilament) 1-5 and TH (tyrosine hydroxylase) by Usoskin et al. Mean
619 expression of *Oprm1,, Scn9a, Scn10a, and Trpv1* was normalized and plotted as a heat map using
620 Graphpad Prism (Figs. S3A and S3B).

621

622 **Data analysis**

623 Data analysis was performed in GraphPad Prism 8.0 (GraphPad Software, Inc., La Jolla, CA).
624 Results for each experiment were expressed as mean ± SEM. The statistical tests used for data analysis
625 are indicated in the text or figure legends. The various tests used were: 2-tailed unpaired Student's t-
626 test, repeated measures one-way ANOVA with Dunnett's post-test, repeated measures two-way ANOVA
627 with Sidak's post-test and ordinary two-way ANOVA with Tukey's post-hoc test. Experiments involving
628 three independent variables were analyzed using three-way ANOVA or mixed-effects (REML) analysis
629 with Tukey's or Sidak's post-hoc test. Data were statistically significant when $P < 0.05$.

630

**Acknowledgements:**

The authors wish to thank David Stevens and Dr. Krista Scoggins for their technical assistance. This study was supported by the National Institute of Health grants: P30 DA033934, R01 DA036975, R01 DA024009

**Authorship Contributions:**

K.H.M., J.C.J. and H.I.A. intellectually conceived and designed the experiments. K.H.M., J.C.J., I.A., S.H., A.K. and M.K. conducted experiments, and K.H.M., J.C.J. and H.I.A. performed data analysis. H.I.A. and W.L.D. supervised the project. K.H.M., H.I.A., J.C.J. and W.L.D. wrote or contributed to the writing of the manuscript and all authors approved.

**Competing Interests:**

The authors declare no conflict of interest or competing financial interests.

643 **References:**


644 Afonso-Pereira F, Dou L, Trenfield SJ, Madla CM, Murdan S, Sousa J, Veiga F, and Basit AW (2018) Sex
645 differences in the gastrointestinal tract of rats and the implications for oral drug delivery. *Eur J*
646 *Pharm Sci*, doi: 10.1016/j.ejps.2018.01.043.

647 Altarifi AA, David B, Muchhala KH, Blough BE, Akbarali H, and Negus SS (2017) Effects of acute and
648 repeated treatment with the biased mu opioid receptor agonist TRV130 (oliceridine) on measures
649 of antinociception, gastrointestinal function, and abuse liability in rodents. *J Psychopharmacol*
650 **31**:730–739.

651 Arttamangkul S, Heinz DA, Bunzow JR, Song X, and Williams JT (2018) Cellular tolerance at the μ-opioid
652 receptor is phosphorylation dependent. *Elife* **7**:1–18.

653 Bailey CP, Smith FL, Kelly E, Dewey WL, and Henderson G (2006) How important is protein kinase C in μ-
654 opioid receptor desensitization and morphine tolerance? *Trends Pharmacol Sci* **27**:558–565.

655 Bardoni R, Tawfik VL, Wang D, François A, Solorzano C, Shuster SA, Choudhury P, Betelli C, Cassidy C,
656 Smith K, DeNooij JC, Mennicken F, O'Donnell D, Kieffer BL, Woodbury CJ, Basbaum AI, MacDermott
657 AB, and Scherrer G (2014) Delta opioid receptors presynaptically regulate cutaneous
658 mechanosensory neuron input to the spinal cord dorsal horn. *Neuron* **81**:1312–1327, Elsevier.

659 Bayguinov O, and Sanders KM (1993) Regulation of neural responses in the canine pyloric sphincter by
660 opioids. *Br J Pharmacol*, doi: 10.1111/j.1476-5381.1993.tb13500.x.

661 Bergese SD, Brzezinski M, Hammer GB, Beard TL, Pan PH, Mace SE, Berkowitz RD, Cochrane K, Wase L,
662 Minkowitz HS, and Habib A (2019) ATHENA: A Phase 3, Open-Label Study Of The Safety And
663 Effectiveness Of Oliceridine (TRV130), A G-Protein Selective Agonist At The μ-Opioid Receptor, In
664 Patients With Moderate To Severe Acute Pain Requiring Parenteral Opioid Therapy. *J Pain Res*
665 **Volume 12**:3113–3126, Dove Press.

666 Bianchetti A, Giudice A, Nava F, and Manara L (1986) Dissociation of Morphine Withdrawl Diarrhea and
667 Jumping in Mice. *Life Sci* **39**:2297–2303.

668 Bodnar RJ, and Kest B (2010) Sex differences in opioid analgesia, hyperalgesia, tolerance and
669 withdrawal: Central mechanisms of action and roles of gonadal hormones. *Horm Behav* **58**:72–81,
670 Elsevier Inc.

671 Bohn LM, Gainetdinov RR, Lin FT, Lefkowitz RJ, and Caron MG (2000) μ-opioid receptor desensitization
672 by β-arrestin-2 determines morphine tolerance but not dependence. *Nature* **408**:720–723, Nature
673 Publishing Group.

674 Bohn LM, Lefkowitz RJ, and Caron MG (2002) Differential mechanisms of morphine antinociceptive
675 tolerance revealed in βarrestin-2 knock-out mice. *J Neurosci* **22**:10494–10500.

676 Bohn LM, Lefkowitz RJ, Gainetdinov RR, Peppel K, Caron MG, and Lin FT (1999) Enhanced morphine
677 analgesia in mice lacking β-arrestin 2. *Science (80- )* **286**:2495–2498.

678 Chen J, Gong ZH, Yan H, Qiao Z, and Qin BY (2012) Neuroplastic alteration of TTX-resistant sodium
679 channel with visceral pain and morphine-induced hyperalgesia. *J Pain Res* **5**:491–502, Dove Press.

680 Chen S-R, Prunean A, Pan H-M, Welker KL, and Pan H-L (2007) Resistance to morphine analgesic
681 tolerance in rats with deleted transient receptor potential vanilloid type 1-expressing sensory
682 neurons. *Neuroscience* **145**:676–85, NIH Public Access.

683 Collier HOJ, Cuthbert NJ, and Francis DL (1981) Model of opiate dependence in the guinea-pig isolated
684 ileum. *Br J Pharmacol* **73**:921–32.

685 Corder G, Doolen S, Donahue RR, Winter MK, Jutras BL, He Y, Hu X, Wieskopf JS, Mogil JS, Storm DR,
686 Wang ZJ, McCarson KE, and Taylor BK (2013) Constitutive μ-opioid receptor activity leads to long-
687 term endogenous analgesia and dependence. *Science (80- )* **341**:1394–1399.

688 Corder G, Tawfik VL, Wang D, Sypek EI, Low SA, Dickinson JR, Sotoudeh C, Clark JD, Barres BA, Bohlen CJ,
689 and Scherrer G (2017) Loss of μ opioid receptor signaling in nociceptors, but not microglia,
690 abrogates morphine tolerance without disrupting analgesia. *Nat Med* **23**:164–173, Nature
691 Publishing Group.

692 Costa M (2000) Anatomy and physiology of the enteric nervous system. *Gut* **47**:15iv – 19.

693 Cox BM (1999) Mechanisms of Tolerance, in *Opioids in Pain Control: Basic and Clinical Aspects* (Stein C
694 ed) pp 109–130, Cambridge University Press, 1999.

695 Dang VC, and Christie MJ (2012) Mechanisms of rapid opioid receptor desensitization, resensitization
696 and tolerance in brain neurons. *Br J Pharmacol* **165**:1704–1716.

697 DeWire SM, Yamashita DS, Rominger DH, Liu G, Cowan CL, Graczyk TM, Chen XT, Pitis PM, Gotchev D,
698 Yuan C, Koblish M, Lark MW, and Violin JD (2013) A G protein-biased ligand at the μ-opioid
699 receptor is potently analgesic with reduced gastrointestinal and respiratory dysfunction compared
700 with morphines. *J Pharmacol Exp Ther* **344**:708–717.

701 Dighe S V., Madia PA, Sirohi S, and Yoburn BC (2009) Continuous morphine produces more tolerance
702 than intermittent or acute treatment. *Pharmacol Biochem Behav* **92**:537–542, Elsevier Inc.

703 Donroe JH, Holt SR, and Tetrault JM (2016) Caring for patients with opioid use disorder in the hospital.
704 *Can Med Assoc J* **188**:1232–1239.

705 Flock T, Hauser AS, Lund N, Gloriam DE, Balaji S, and Babu MM (2017) Selectivity determinants of GPCR-
706 G-protein binding. *Nature* **545**:317–322, Nature Publishing Group.

707 Furness JB, Callaghan BP, Rivera LR, and Cho H-J (2014) The Enteric Nervous System and Gastrointestinal
708 Innervation: Integrated Local and Central Control, in pp 39–71, Springer, New York, NY.

709 Gabra BH, Bailey CP, Kelly E, Smith FL, Henderson G, and Dewey WL (2008) Pre-treatment with a PKC or
710 PKA inhibitor prevents the development of morphine tolerance but not physical dependence in
711 mice. *Brain Res* **1217**:70–77, Elsevier.

712 Gold MS, Reichling DB, Shuster MJ, and Levine JD (1996) Hyperalgesic agents increase a tetrodotoxin-
713 resistant Na+ current in nociceptors. *Proc Natl Acad Sci U S A* **93**:1108–1112, National Acad
714 Sciences.

715 Grim TW, Schmid CL, Stahl EL, Pantouli F, Ho J-H, Acevedo-Canabal A, Kennedy NM, Cameron MD,
716 Bannister TD, and Bohn LM (2020) A G protein signaling-biased agonist at the μ-opioid receptor

717 reverses morphine tolerance while preventing morphine withdrawal. *Neuropsychopharmacology*
718 **45**:416–425.

719 Harris LS, and Pierson AK (1964) Some Narcotic Antagonists In The Benzomorphan Series. *J Pharmacol*
720 *Exp Ther* **143**:141–148.

721 Hayhurst CJ, and Durieux ME (2016) Differential Opioid Tolerance and Opioid-induced Hyperalgesia: A
722 Clinical Reality, Lippincott Williams and Wilkins.

723 Hertz S (2018) FDA Briefing Document Anesthetic and Analgesic Drug Products Advisory Committee
724 (AADPAC) Meeting. 1–115.

725 Hilger D, Masureel M, and Kobilka BK (2018) Structure and dynamics of GPCR signaling complexes. *Nat*
726 *Struct Mol Biol* **25**:4–12, Nature Publishing Group.

727 Holzer P (2009) Opioid receptors in the gastrointestinal tract. *Regul Pept* **155**:11–17, Elsevier B.V.

728 Hua X-Y, Moore A, Malkmus S, Murray SF, Dean N, Yaksh TL, and Butler M (2002) Inhibition of spinal
729 protein kinase Cα expression by an antisense oligonucleotide attenuates morphine infusion-
730 induced tolerance. *Neuroscience* **113**:99–107, Elsevier.

731 Inoue M, and Ueda H (2000) Protein kinase C-mediated acute tolerance to peripheral μ-opioid analgesia
732 in the bradykinin-nociception test in mice. *J Pharmacol Exp Ther* **293**:662–669, ASPET.

733 Jacob JC, Sakakibara K, Mischel RA, Henderson G, Dewey WL, and Akbarali HI (2018) Ethanol reversal of
734 oxycodone tolerance in dorsal root ganglia neurons. *Mol Pharmacol* **93**:417–426.

735 Johnson SM, Humphreys CMS, and Costa M (1987) Sustained nerve-mediated contractions of guinea-pig
736 ileum during morphine withdrawal by washout. *Eur J Pharmacol* **141**:41–50.

737 Kang M, Maguma HT, Smith TH, Ross GR, Dewey WL, and Akbarali HI (2012) The role of β-arrestin2 in
738 the mechanism of morphine tolerance in the mouse and guinea pig gastrointestinal tract. *J*
739 *Pharmacol Exp Ther* **340**:567–576, American Society for Pharmacology and Experimental
740 Therapeutics.

741 Katakami N, Harada T, Murata T, Shinozaki K, Tsutsumi M, Yokota T, Arai M, Tada Y, Narabayashi M, and
742 Boku N (2018) Randomized phase III and extension studies: Efficacy and impacts on quality of life
743 of naldemedine in subjects with opioid-induced constipation and cancer. *Ann Oncol*, doi:
744 10.1093/annonc/mdy118.

745 Katakami N, Harada T, Murata T, Shinozaki K, Tsutsumi M, Yokota T, Arai M, Tada Y, Narabayashi M, and
746 Boku N (2017) Randomized phase III and extension studies of naldemedine in patients with opioid-
747 induced constipation and cancer. *J Clin Oncol*, doi: 10.1200/JCO.2017.73.0853.

748 Kenakin T (2011) Functional selectivity and biased receptor signaling.

749 Kimball ES, Palmer JM, D'Andrea MR, Hornby PJ, and Wade PR (2005) Acute colitis induction by oil of
750 mustard results in later development of an IBS-like accelerated upper GI transit in mice. *Am J*
751 *Physiol Gastrointest Liver Physiol* **288**:G1266-73.

752 Kliewer A, Schmiedel F, Sianati S, Bailey A, Bateman JT, Levitt ES, Williams JT, Christie MJ, and Schulz S
753 (2019) Phosphorylation-deficient G-protein-biased μ-opioid receptors improve analgesia and

754 diminish tolerance but worsen opioid side effects. *Nat Commun* **10**:367.

755 Latorraca NR, Venkatakrishnan AJ, and Dror RO (2017) GPCR dynamics: Structures in motion, American
756 Chemical Society.

757 Lee CWS, and Ho IK (2013) Sex differences in opioid analgesia and addiction: Interactions among opioid
758 receptors and estrogen receptors. *Mol Pain* **9**:1–10.

759 Lefkowitz RJ (1998) G protein-coupled receptors: III. New roles for receptor kinases and β- arrestins in
760 receptor signaling and desensitization.

761 Levitt ES, and Williams JT (2012) Morphine desensitization and cellular tolerance are distinguished in rat
762 locus ceruleus neurons. *Mol Pharmacol*, doi: 10.1124/mol.112.081547.

763 Li Z, Chalazonitis A, Huang Y-Y, Mann JJ, Margolis KG, Yang QM, Kim DO, Côté F, Mallet J, and Gershon
764 MD (2011) Essential roles of enteric neuronal serotonin in gastrointestinal motility and the
765 development/survival of enteric dopaminergic neurons. *J Neurosci* **31**:8998–9009.

766 Ling GSF, Paul D, Simantov R, and Pasternak GW (1989) Differential development of acute tolerance to
767 analgesia, respiratory depression, gastrointestinal transit and hormone release in a morphine
768 infusion model. *Life Sci* **45**:1627–1636.

769 Lohse MJ, Benovic JL, Codina J, Caron MG, and Lefkowitz RJ (1990) beta-Arrestin: a protein that
770 regulates beta-adrenergic receptor function. *Science (80- )* **248**:1547–1550, American Association
771 for the Advancement of Science.

772 Ma RSY, Kayani K, Whyte-Oshodi D, Whyte-Oshodi A, Nachiappan N, Gnanarajah S, and Mohammed R
773 (2019) Voltage gated sodium channels as therapeutic targets for chronic pain. *J Pain Res* **12**:2709–
774 2722.

775 Madariaga-Mazón A, Marmolejo-Valencia AF, Li Y, Toll L, Houghten RA, and Martinez-Mayorga K (2017)
776 Mu-Opioid receptor biased ligands: A safer and painless discovery of analgesics?

777 Maguma HT, Dewey WL, and Akbarali HI (2012) Differences in the characteristics of tolerance to μ-
778 opioid receptor agonists in the colon from wild type and β-arrestin2 knockout mice. *Eur J*
779 *Pharmacol* **685**:133–140, Elsevier B.V.

780 Manglik A, Lin H, Aryal DK, McCorvy JD, Dengler D, Corder G, Levit A, Kling RC, Bernat V, Hübner H,
781 Huang XP, Sassano MF, Giguère PM, Löber S, Duan D, Scherrer G, Kobilka BK, Gmeiner P, Roth BL,
782 and Shoichet BK (2016) Structure-based discovery of opioid analgesics with reduced side effects.
783 *Nature* **537**:185–190, Nature Publishing Group.

784 McLane VD, Bergquist I, Cormier J, Barlow DJ, Houseknecht KL, Bilsky EJ, and Cao L (2017) Long-term
785 morphine delivery via slow release morphine pellets or osmotic pumps: Plasma concentration,
786 analgesia, and naloxone-precipitated withdrawal. *Life Sci* **185**:1–7, Elsevier Inc.

787 Michel MC, and Charlton SJ (2018) Biased agonism in drug discovery-is it too soon to choose a path? *Mol*
788 *Pharmacol* **93**:259–265.

789 Mischel RA, Dewey WL, and Akbarali HI (2018) Tolerance to Morphine-Induced Inhibition of TTX-R
790 Sodium Channels in Dorsal Root Ganglia Neurons Is Modulated by Gut-Derived Mediators. *iScience*

791 **2**:193–209, Elsevier.

792 Pines A, Eckstein N, Dotan I, Ayalon D, Varon D, Barnea O, and Shavit G (1998) Effect of estradiol on rat
793 ileum. *Gen Pharmacol* **31**:735–736.

794 Raehal KM, Walker JKL, and Bohn LM (2005) Morphine side effects in β-arrestin 2 knockout mice. *J*
795 *Pharmacol Exp Ther* **314**:1195–1201.

796 Rajagopal S, Ahn S, Rominger DH, Gowen-MacDonald W, Lam CM, DeWire SM, Violin JD, and Lefkowitz
797 RJ (2011) Quantifying ligand bias at seven-transmembrane receptors. *Mol Pharmacol* **80**:367–377.

798 Ross GR, Gabra BH, Dewey WL, and Akbarali HI (2008) Morphine tolerance in the mouse ileum and
799 colon. *J Pharmacol Exp Ther* **327**:561–572.

800 Shekunova E V., and Bespalov AY (2006) Effects of memantine on estrogen-dependent acute tolerance
801 to the morphine analgesia in female rats. *Eur J Pharmacol*, doi: 10.1016/j.ejphar.2006.02.020.

802 Shekunova E V., and Bespalov AY (2004) Estrous cycle stage-dependent expression of acute tolerance to
803 morphine analgesia in rats. *Eur J Pharmacol*, doi: 10.1016/j.ejphar.2004.01.012.

804 Siuda ER, Carr R, Rominger DH, and Violin JD (2017) Biased mu-opioid receptor ligands: a promising new
805 generation of pain therapeutics.

806 Smith FL, Javed RR, Elzey MJ, and Dewey WL (2003) The expression of a high level of morphine
807 antinociceptive tolerance in mice involves both PKC and PKA. *Brain Res* **985**:78–88, Elsevier.

808 Smith FL, Javed RR, Smith PA, Dewey WL, and Gabra BH (2006) PKC and PKA inhibitors reinstate
809 morphine-induced behaviors in morphine tolerant mice. *Pharmacol Res* **54**:474–80, Elsevier.

810 Smith FL, Lohmann AB, and Dewey WL (1999) Involvement of phospholipid signal transduction pathways
811 in morphine tolerance in mice. *Br J Pharmacol* **128**:220–226, Wiley Online Library.

812 Smith TH, Grider JR, Dewey WL, and Akbarali HI (2012) Morphine Decreases Enteric Neuron Excitability
813 via Inhibition of Sodium Channels. *PLoS One* **7**:e45251, Public Library of Science.

814 Smith TH, Ngwainmbi J, Grider JR, Dewey WL, and Akbarali HI (2013) An in-vitro preparation of isolated
815 enteric neurons and glia from the myenteric plexus of the adult mouse. *J Vis Exp*, doi:
816 10.3791/50688, MyJoVE Corporation.

817 Smith TH, Ngwainmbi J, Hashimoto A, Dewey WL, and Akbarali HI (2014) Morphine dependence in single
818 enteric neurons from the mouse colon requires deletion of β -arrestin2. *Physiol Rep* **2**:e12140.

819 Sorge RE, Martin LJ, Isbester KA, Sotocinal SG, Rosen S, Tuttle AH, Wieskopf JS, Acland EL, Dokova A,
820 Kadoura B, Leger P, Mapplebeck JCS, McPhail M, Delaney A, Wigerblad G, Schumann AP, Quinn T,
821 Frasnelli J, Svensson CI, Sternberg WF, and Mogil JS (2014) Olfactory exposure to males, including
822 men, causes stress and related analgesia in rodents. *Nat Methods* **11**:629–632.

823 Sun J, Chen SR, Chen H, and Pan HL (2019) μ-Opioid receptors in primary sensory neurons are essential
824 for opioid analgesic effect on acute and inflammatory pain and opioid-induced hyperalgesia. *J*
825 *Physiol* **597**:1661–1675.

826 Usoskin D, Furlan A, Islam S, Abdo H, Lönnerberg P, Lou D, Hjerling-Leffler J, Haeggström J, Kharchenko

827 O, Kharchenko P V, Linnarsson S, and Ernfors P (2015) Unbiased classification of sensory neuron
828 types by large-scale single-cell RNA sequencing. *Nat Neurosci* **18**:145–53.

829 Wang J, Xu W, Zhong T, Song Z, Zou Y, Ding Z, Guo Q, Dong X, and Zou W (2016) MiR-365 targets β-
830 arrestin 2 to reverse morphine tolerance in rats. *Sci Rep* **6**:1–11.

831 Wang L, Medina VM, Rivera M, and Gintzler AR (1996) Relevance of phosphorylation state to opioid
832 responsiveness in opiate naive and tolerant/dependent tissue. *Brain Res*, doi: 10.1016/0006-
833 8993(96)00217-X.

834 Warhurst G, Smith GS, Higgs N, Tonge A, and Turnberg LA (1984) Influence of Morphine Tolerance and
835 Withdrawal on Intestinal Salt and Water Transport in the Rat In Vivo and In Vitro. *Gastroenterology*
836 **87**:1035–1041, American Gastroenterological Association.

837 Wesson DR, and Ling W (2003) The Clinical Opiate Withdrawal Scale (COWS). *J Psychoactive Drugs*
838 **35**:253–259.

839 Williams JT, Ingram SL, Henderson G, Chavkin C, von Zastrow M, Schulz S, Koch T, Evans CJ, and Christie
840 MJ (2013) Regulation of μ-opioid receptors: Desensitization, phosphorylation, internalization, and
841 tolerance. *Pharmacol Rev* **65**:223–254.

842 Withey SL, Hill R, Lyndon A, Dewey WL, Kelly E, and Henderson G (2017) Effect of tamoxifen and brain-
843 penetrant protein kinase C and c-Jun N-terminal kinase inhibitors on tolerance to opioid-induced
844 respiratory depression in mice. *J Pharmacol Exp Ther* **361**:51–59.

845 Wootten D, Christopoulos A, Marti-Solano M, Babu MM, and Sexton PM (2018) Mechanisms of
846 signalling and biased agonism in G protein-coupled receptors. *Nat Rev Mol Cell Biol* **19**:638–653,
847 Springer US.

848 Yang CH, Huang HW, Chen KH, Chen YS, Sheen-Chen SM, and Lin CR (2011) Antinociceptive potentiation
849 and attenuation of tolerance by intrathecal β-arrestin 2 small interfering RNA in rats. *Br J Anaesth*
850 **107**:774–781, British Journal of Anaesthesia. Published by Elsevier Ltd.

851 Zeisel A, Hochgerner H, Lönnerberg P, Johnsson A, Memic F, van der Zwan J, Häring M, Braun E, Borm LE,
852 La Manno G, Codeluppi S, Furlan A, Lee K, Skene N, Harris KD, Hjerling-Leffler J, Arenas E, Ernfors P,
853 Marklund U, and Linnarsson S (2018) Molecular Architecture of the Mouse Nervous System. *Cell*
854 **174**:999-1014.e22.

855

856

857
858
859
860
861
862
863
864
865

**Supplementary Tables and Figures**

| Related to Figure ## | | Main effect | F (DFn, DFd) | P value |
|---|---|---|---|---|
| 1 | A | Cumulative morphine dose x Sex x Pellet pre-treatment on tail-withdrawal % MPE | F (8, 112) = 13.74 | <0.0001 |
| | B | Cumulative morphine dose x Pellet pre-treatment on tail-withdrawal % MPE | F (8, 80) = 7.477 | <0.0001 |
| 3 Ileum neurons | A | Pre-treatment x Acute morphine challenge on βarr2 WT Ileum $V_{thresh}$ | F (2, 16) = 24.55 | <0.0001 |
| | B | Pre-treatment x Acute morphine exposure time on βarr2 WT Ileum $V_{thresh}$ | F (16, 104) = 1.892 | 0.0292 |
| | C | Pre-treatment x Acute morphine challenge on βarr2 KO Ileum $V_{thresh}$ | F (2, 17) = 21.51 | <0.0001 |
| | D | Pre-treatment x Acute morphine exposure time on βarr2 KO Ileum $V_{thresh}$ | F (16, 136) = 2.042 | 0.0145 |
| | E | Pre-treatment x Genotype on $V_{thresh}$ change | F (2, 33) = 1.498 | 0.2383 |
| 4 Male SI Transit | A | Pellet pre-treatment x Genotype | F (1, 19) = 0.02683 | 0.8716 |
| | B | Pellet pre-treatment x Genotype | F (1, 19) = 0.1816 | 0.6748 |
| | C | Pellet pre-treatment x Genotype | F (1, 26) = 1.584 | 0.2194 |
| | D | Pellet pre-treatment x Genotype | F (1, 30) = 2.727 | 0.1091 |
| 5 Female SI Transit | A | Pellet pre-treatment x Genotype | F (1, 15) = 5.019 | 0.0406 |
| | B | Pellet pre-treatment x Genotype | F (1, 22) = 0.8978 | 0.3537 |
| 6 | A | Pellet pre-treatment x Acute tamoxifen challenge on charcoal transit | F (1, 24) = 27.75 | <0.0001 |
| | B | Bis XI x Acute morphine challenge on $V_{thresh}$ of ileum neurons | F (1, 12) = 19.77 | 0.0008 |

| | | | | |
|---|---|---|---|---|
| **7** | **A** | Days exposed to morphine pellet on tail-withdrawal latency | F (1.9, 15.5) = 62.14 | <0.0001 |
| | **B** | Pellet pre-treatment x Acute challenge on tail-withdrawal % MPE | F (1, 16) = 1.740 | 0.2057 |
| | **C** | Pellet pre-treatment x Acute challenge on % charcoal transit | F (1, 16) = 147.2 | <0.0001 |
| **8** | **A** | Days exposed to pellet x pellet pre-treatment | F (7, 104) = 17.56 | <0.0001 |
| | **B** | Days exposed to pellet x pellet pre-treatment | F (5, 65) = 14.48 | <0.0001 |

**Table S1. Figure-wise results highlighting the main effect of ANOVA analyses.**
SI=Small Intestine; TW=Tail-withdrawal

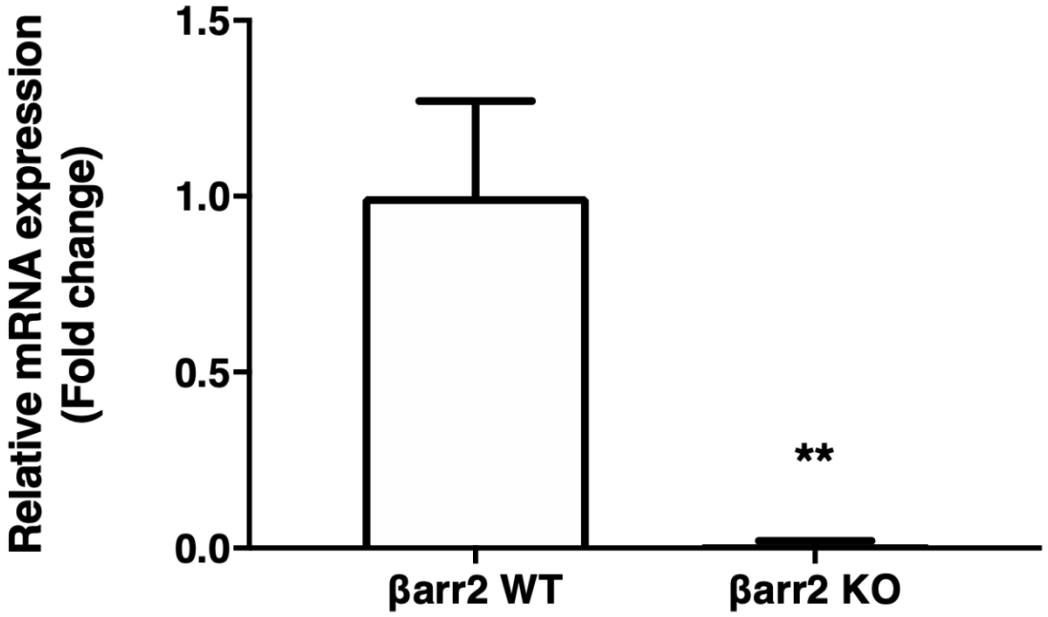


**Figure S1. Relative expression of mouse β-arrestin-2 mRNA normalized to mouse 18S.** Expression of βarr2 extracted from spinal cord of naïve βarr2 WT and KO male mice. N=4 mice/group; n=8, including technical repeats. **P<0.01 (versus βarr2 WT) by two-tailed unpaired t-test (t=3.664, df=14). Line and error are mean ± SEM.

A

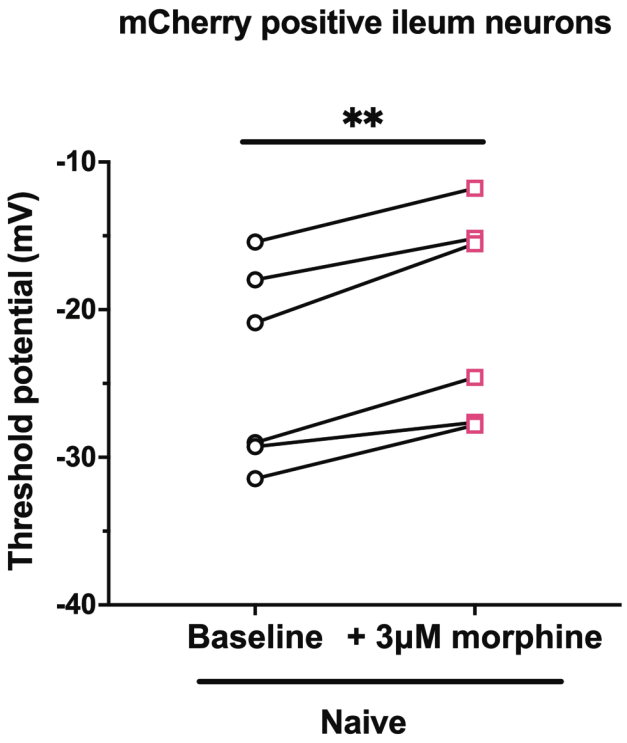


B

| $V_{thresh}$ | Ileum neurons |
|---|---|
| **Baseline** | -24.0 ± 2.8 mV |
| **+ 3 μM morphine** | -20.42 ± 2.9 mV |

**Figure. S2. Acute morphine increased threshold potential of mCherry-positive ileum myenteric plexus neurons.** (A) 3 μM morphine increased the threshold to fire action potential in mCherry-positive ileum myenteric plexus neurons. *P<0.05 and **P<0.01 by two-tailed paired t-test. All mCherry-positive ileum neurons exhibited after-hyperpolarization. (B) Action potential threshold in mCherry-positive neurons at baseline and after 3 μM morphine exposure. Values are mean ± SEM.

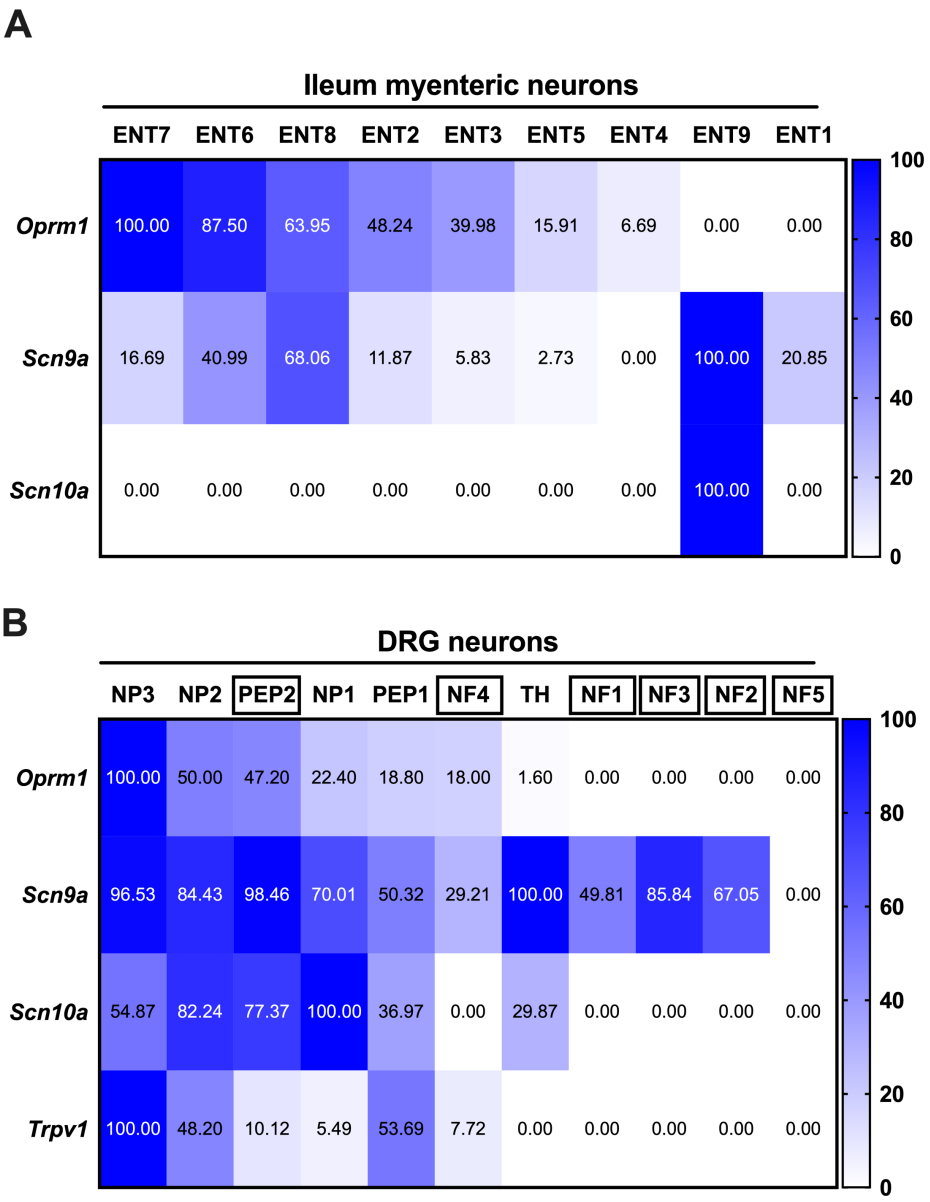


**Figure S3. Gene expression profile of select transcripts in naïve mouse ileum and DRG neurons.** Heat maps of normalized gene expression in (A) ileum myenteric plexus and (C) L4-L6 DRG neuron clusters. Correlation heat maps of genes of interest in (B) ileum myenteric and (D) DRG neurons. Single-cell RNA seq data of the mouse (A, B) ileum myenteric plexus and (C, D) DRG was obtained from Zeisel et al., 2018 and Usoskin et al., 2015, respectively. (C) '□' indicates the presence of myelination in DRG neuron subsets. Gene data was normalized to the cluster expressing the most transcript.